LICENCE TO McMASTER UNIVERSITY

This THESIS has been written
[Thesis, Project Report, etc.]

by KATHLEEN JOAN GLADYSZ for
[Full Name(s)]
Undergraduate course number GEOG 4C6 at McMaster University under the supervision/direction of DR. DEREK C. FORD.

In the interest of furthering teaching and research, I/we hereby grant to McMaster University:

1. The ownership of ONE copy(ies) of this work;
2. A non-exclusive licence to make copies of this work, (or any part thereof) the copyright of which is vested in me/us, for the full term of the copyright, or for so long as may be legally permitted. Such copies shall only be made in response to a written request from the Library or any University or similar institution.

I/we further acknowledge that this work (or a surrogate copy thereof) may be consulted without restriction by any interested person.

Signature of Witness, Supervisor

Kathleen Gladysz
Signature of Student

APRIL 10, 1987
date

(This Licence to be bound with the work)

KARREN ON QUATSINO FM. DIP SLOPES RECENTLY EXPOSED BY DEFORESTATION NORTHERN VANCOUVER ISLAND

KATHLEEN JOAN GLADYSZ

A Research Paper
Submitted to the Department of Geography
in Fulfilment of the Requirements
of Geog 4C6

McMaster University
April 1987

ABSTRACT

This study reports on karren forms on limestone dip slopes, which were recently exposed by deforestation on the Quatsino Formation and observable relationships of the karren features of a specific slope are represented as a detailed map. Also, many relationships of gravitomorphic runnel characteristics are analyzed for significance. Runnel types being considered are Hortonian, decantation and composite forms. Solution runnel width, depth and width/depth ratio are studied in association with length. These relationships determine whether the runnel types conform to a theoretical model. Typical measures of the karren in this area were also recorded. Composite forms are the most abundant because Hortonian and decantation runnels amalgamate beyond about 3m to form composites. All the runnel types, excluding the decanters, illustrate the perfect minimum friction open-channel cross-section.

ACKNOWLEDGEMENTS

I wish to express my sincere thanks to Dr. D.C. Ford for his constant advice, support and encouragement throughout this study; Joyce Lundberg for her advice and valuable assistance in Dr. Ford's absence; Ric Hamilton for his expertise in cartographic techniques, friendship and a smile. Kathleen Harding and Brenda Stephan, thank you for your invaluable companionship, assistance in the field and the memorable moments in Port Alice, B.C. A smile means so much.

TABLE OF CONTENTS

LIST OF FIGURES

LIST OF TABLES

Block D-E of the main site illustrating well-developed Rundkarren which resemble those of Hatton Roof, England. On the lower part of the slope fractures dominate. Regrowth in the dips is healthy. Large tree stumps indicate the former tree cover on the now bare rock slopes.

CHAPTER ONE

INTRODUCTION AND LITERATURE REVIEW

1.1 INTRODUCTION

Small-scale solutional features (karren) are common on limestones. The purpose of this study is to report on karren forms on limestone dip slopes, which were recently exposed by deforestation on the Quatsino Formation on northern Vancouver Island. The karren under consideration are fractures, gravity controlled linear features and lapies wells.

Fracture controlled features develop on small fractures or joints. Kluftkarren are solutionally widened joints, also known as grikes. It is along these lines of weakness that the greatest solution occurs (Sweeting, 1973). Grikes form on both bare karst and beneath a soil cover (Bogli, 1980). On Vancouver Island they are straight, narrow, long and deep. Enlargement and rounding may occur at joint intersections producing lapies wells. Both grikes and lapies wells take water underground.

Gravity controlled features trend downslope and may

be of Hortonian type or decantation type. In this area Rundkarren and rinnenkarren were the observed Hortonian type channels. These are solution runnels which generally increase in width and depth downslope, due to the accumulation of larger volumes of water. Rinnenkarren develop on bare rock and their edges are sharp. Rundkarren develop under a cover. Their troughs, crests and sides are smooth and rounded. The distinctions are shown in Figure 1.1 (See Appendix A). This rounding results from the modification of solution by the cover, typically an acid soil. They generally are revealed when a cover has been removed. Rundkarren and rinnenkarren behave like river channels. They usually show a typical dendritic pattern, but on steeper slopes will tend to be sub-parallel (Sweeting, 1973).

Decantation runnels occur where water is released onto the slope from a store. This store may be moss or humic material which retains water and discharges it upon saturation. Thus, since the most aggressive water exists at the store, the runnel is deepest there and shallows downslope.

In this study the relationships of the karren forms are to be examined and displayed by detailed mapping; then the field measures of morphometric characteristics of the gravity controlled features will provide the necessary data

to test various hypotheses. For example, one may hypothesize that the width and depth of the features are related, or that significant relationships exist between width, depth and the W/D ratio with respect to length.

1.2 LITERATURE REVIEW

The karren studied were rinnenkarren, rundkarren, decantation forms and kluftkarren. Rinnenkarren occur where water flows unhindered over the surface and the amount of water is sufficient to form streams (Bogli,1960,1980; Sweeting, 1973; Jennings, 1985; Ford and Lundberg (in press)). Rinnenkarren increase in width and depth downslope in accordance with the uniform addition of water. They have sharp channel rims and rounded bases. Their dimensions are highly variable. Sweeting (1973) quotes depths up to 50 cm and lengths up to 20 m. Rinnenkarren are common in the Alps, the Dinaric karst and other mountainous regions where bare limestone slopes predominate. In Lapland, snow and glacial meltwater flowing over limestones has formed distinct rinnenkarren (Sweeting, 1973). As these are snow and meltwater features, they are more likely to be decantation forms, or simply stream channels with abrasive material flowing through them.

Bogli (1960) believed rinnenkarren to be formed during Phase 4 of the limestone solution process. Those parts of the reaction which are rate controlled by the

physical dissolution of calcium carbonate and by the dissolved carbon dioxide have been completed. This final phase controls further solution to the end of the process. Carbon dioxide in the air diffuses into the water and initiates a reaction sequence. This will continue as long as calcium carbonate can be dissolved. The diffusion rate determines the time to completion. The material conversion rate and therefore the intensity of solution are quite small, and decreasing.

Rundkarren are rounded solution runnels which are generally observed where a soil cover has been removed (Ford and Lundberg, in press). These features are similar in size to rinnenkarren, being about 12 - 50 cm wide, and they may enlarge downslope.

Opinions have varied on the origin of rundkarren. Sweeting (1973) believed them to be drainage features developed beneath a peat or vegetation cover. It was suggested by Bogli (1960) that although the usual type forms under a cover sometimes rundkarren are actually complex rinnenkarren. In humid climates limestones eventually become covered by vegetation. Consequently, the aggressive environment at the soil-rock interface causes the sharp corners to be rounded off.

A vegetation/soil cover may have a significant effect on limestone solution. The free flow of water is

inhibited resulting in an extended reaction between the water, with its biogenic CO_2, and the rock. While the water remains in the soil zone it becomes enriched with CO_2. This aggressive water dissolves all available $CaCO_3$ and eventually attacks the underlying bedrock. Consequently, all karren formed beneath a vegetation cover are of the rounded varieties. Therefore, the presence of rundkarren in a currently bare area is an indication of a former vegetation cover. The direct action of plant roots and soil upon the limestone must also be considered (Bogli, 1960;1980). Trudgill demonstrated the relationship between soil characteristics and the rate of bedrock erosion: Calcareous soils protect the bedrock while erosional modification occurs under acid soils (1976e and 1985). Rainwater has considerably less dissolution potential than acid soil water. Jones (1965) asserted that the solution of limestone by soil water is of much greater importance than the action of rainwater and that soil-covered surfaces are more deeply eroded than bare limestone. Surfaces which are covered with acid soil suffer a corrosive soaking whereas soil free surfaces are exposed only to episodic dissolution events under the action of rainwater. The solution potential of acidic soil waters is indicated by the study of solution forms of a tropical granodiorite terrain in Puerto Rico conducted by Beck and Cram (1977). Their research

indicated that the features resulted from a previous vegetative cover.

Decantation runnels occur where water is released onto the slope from a store. This store may be moss or humic material which retains water and discharges it upon saturation. Similar to water retained in a vegetative cover, this water may become more aggressive during storage. The diagnostic characteristic of decantation forms is their tendency to become shallower downslope because the most aggressive water exists at the store, and so the runnel is deepest immediately beyond it. As they may not collect water downslope, they become shallower and will eventually extinguish if the slope is long enough.

Decantation runnels have recently been classified by Ford and Lundberg (in press). The most common decantation feature (and the one in this study) is where overspill is from separate point sources. Each spill forms a separate channel. These correspond to wandkarren (Bogli, 1960). The channel dimensions are dependent upon the amount of water overspilling and its aggressivity. Thus, decantation channels may vary widely in size. The other forms (not studied here) occur where overspill in a sheet form produces a suite of parallel flutings.

In reality, decantation and direct rainwater forms tend to be intermixed. For example, a rundkarren may

contain a store of moss. Immediately downslope of the store the overdeepened rill is formed both by rainwater and by decantation effects (Ford and Lundberg, in press). The junction of tributaries and distributaries with the main channel also results in the formation of composite runnel features. The junction of a tributary may result in the deepening and widening of the runnel prematurely. A distributary may cause a decrease in width and depth due to loss of water flow volume beyond the junction. Composite features are frequently observed on the Quatsino Formation limestones of Vancouver Island (Figure 1.2 and 1.3).

Kluftkarren are solutionally widened joints also known as grikes. These features may form both beneath a soil cover and on bare rock. Bogli (1960) suggested that kluftkarren were originally tectonically formed fractures. He estimated their origin to be prior to the last Pleistocene glaciation, as they were "always" truncated by glacial surfaces. This is not necessarily true. For example, Scar Close in Lancashire, and areas of the Bruce Peninsula show both preglacial and postglacial grikes (Lundberg, pers. comm.). Kluftkarren occur in most karst areas of the world. Grikes measured in Yorkshire vary from about 15 cm to about 60 cm wide, and they may be up to 5 m deep. In the Clare-Galway area of Ireland, the grikes tend to average about 24 cm wide and about 1 m deep. The

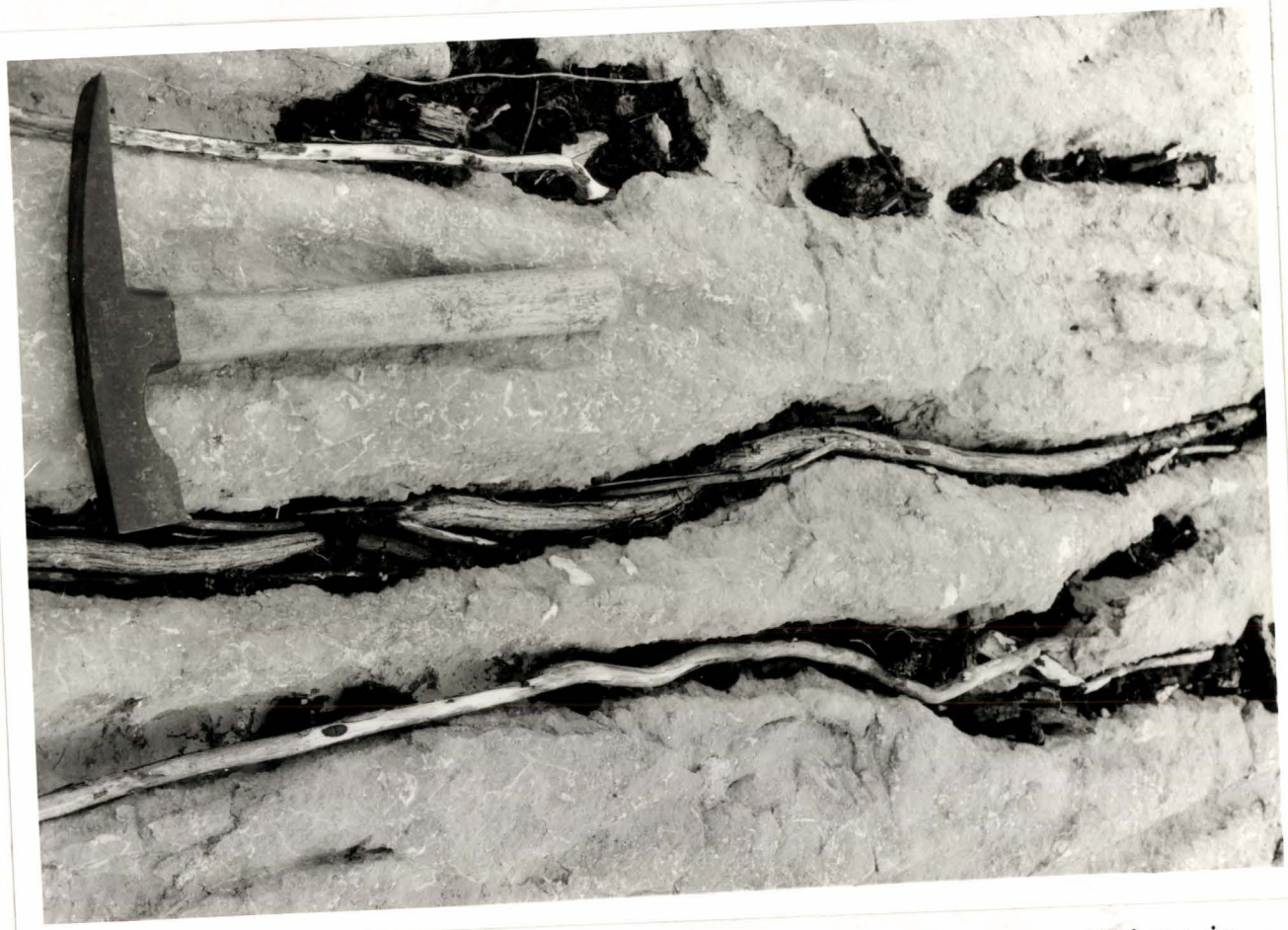

Figure 1.2: Tree roots and moss take advantage of the damper conditions in the runnels. Water is also stored in humic materials

Figure 1.3: Hortonian (example A) and composite (example B) rundkarren.

ir rsection of two or more joints may promote additional s(ıtion. As a result, well-like rounded hollows up to over 5 deep may form. These are termed lapies wells (Sweeting, 1 3).

Gravitomorphic rills of Hortonian and decantation t e may have distinctly different profiles, as noted in F ure 1.4 (See Appendix A). The Hortonian type, r nenkarren and rundkarren, head below a belt of no (nnelled erosion and increase in width and depth (vnslope. They form similarly to rills developing on a il covered hillside. As rain falls the depth of flow wnslope from the crest increases until the flow separates to linear streams. The runnels carrying these streams are uivalent to Horton's first order rills. The planar lution slope may also be defined as the belt of no annelled erosion. Hortonian type runnels increase in dth and depth downslope as the flow increases. They often eet to form larger single channels.

Karren features have been widely studied in escriptive terms. The many factors which affect their evelopment and the environmental changes which occur ndicate that careful identification is very important. orphometric analysis of these features should also be onsidered for further study.

CHAPTER TWO

STUDY SITE AND METHODOLOGY

2 STUDY SITE

This study is of an outcrop of the Quatsino :rmation limestone in northwestern Vancouver Island ig.2.1, Appendix A). The dip slopes of interest to this per are situated along the south side of Kathleen Lake, rth of the Benson River (Figure 2.2). The limestone opes have elevations of 150m to 300m, and strike at about ^{o} '5 NW with predominant dips of 35 ^{o} -40 ^{o}. The slopes ave a similar aspect of 185 ^{o} SW. The mapped section onsists of a slope surface 80 metres wide by 10 metres ownslope length. As the presence and morphometric haracteristics of micro-solutional karren features are eing investigated, certain environmental factors such as :limate lithology, soil type and vegetation must be :onsidered.

2.1.1 CLIMATE

Northwestern Vancouver Island experiences a cool mesothermal climate. The coastal zone is dominated by the flow of air from the Pacific Ocean. This cool air keeps the coast relatively cool in the summer, while in the winter it contributes to temperatures that are mild compared to those

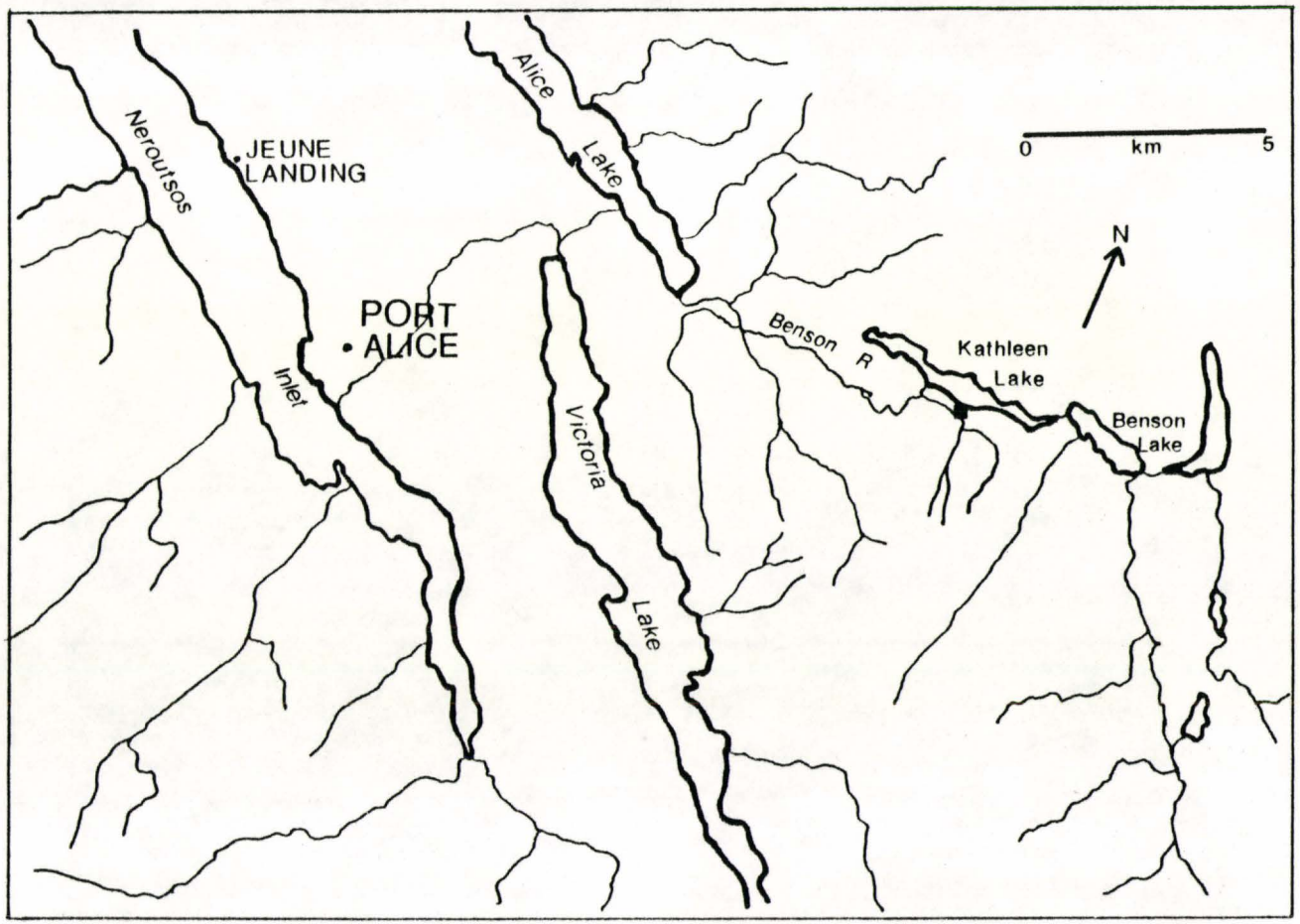

Figure 2.2: Study site: south of Kathleen Lake

i: he interior. This region has a mean annual temperature o about 7 C. The mean monthly temperature ranges from 1 C o 14 C (Mills, 1981; National Atlas of Canada, 1974).

The region receives about 200 days with p cipitation annually. Winters are quite wet due to f quent mid-latitude cyclonic storms, strong air flows, and m ntains in the path of air flow. During the summer p ssure gradients are weaker and air flow is gentler, r ulting in fewer days with measurable precipitation. The m n annual precipitation rate is about 2500 mm/yr, but less t n 500 mm/yr occurs between April and September.

.2 LITHOLOGY

The Quatsino Formation is composed of Upper Triassic 0 - 195 ma BP), (Tozer, 1967) carbonate, pelitic and caniclastic sediments and is the principle carbonate unit the Vancouver Group. These sedimentary rocks outcrop ng valley bottoms in the western zone of the Vancouver land Range (Fig. 2.3, in Appendix A). The unit is exposed three, fault dissected, linear belts which trend minantly northwest-southeast. Karst development occurs imarily along 30 km of the strike aligned Benson River lley and on the adjacent Gibson Plateau. The biomicritic mestones display a bimodal size distribution, dominantly mposed of coral and pelecypod debris in a volumetrically minant matrix of fine carbonate muds. The base of the

s uence consists of dark grey to black coarsely crystalline s ata. These are thick-bedded or massive and commonly d play stylolites. The upper portion of the Quatsino F mation consists of medium to thick-bedded limestones, i erlaminated with black calcareous siltstones (Mills, 1 1).

.3 SOIL TYPE AND VEGETATION

The regional soil type is a Humo-ferric podzol haracterized by an accumulation of organic matter in the soil due to extreme leaching. However, in much of the st soil development is skeletal and influenced by local ctors. The soil temperature regime is cool boreal with a ort warm period. The soil moisture regime, modified by e Maritime influence, is dominantly humid to perhumid.

This region of Vancouver Island occurs in the cific coast and Interior Mid Latitude forest zone. The minant tree species are Douglas Fir, Western Hemlock and e Western Red Cedar (Mills, 1981; National Atlas of nada, 1974). The main study area was deforested and rned in 1970. It appears that many of the valleys between e dip and scarp slopes were replanted in 1971 and are now ll vegetated while the intervening slopes are bare of both oil and vegetation. The severe burn inhibited regrowth so hat the remaining soil, following the burn, was removed by

t natural elements of wind and rainfall.

2 METHODOLOGY

2 1 FIELD SURVEY

Data was collected (i) to enable the production of a d ailed map of the chief section studied and (ii) to e: nine certain morphometric relationships of small-scale k: en features. The 80 metre wide dip slope face to be m ed was divided into eight blocks, ten metres wide, l: lled A to I. Profile measurements of strike, dip, a: ct and downslope length were recorded at each label.

The solutional features were measured with respect t the block in which they were situated. Thus, the p tion of these forms was determined by their distance d slope from the slope crest, and their distance from the s of that particular block. Measurements of morphometric c acteristics were then carefully recorded. Measurements t n for lapies wells were width, depth, downslope length a orientation. Fractures were measured at one metre i rvals of their length, noting distance downslope, width a depth. Solutional runnel measures consisted of length, w h and depth at approximately 20 cm intervals. O ntation and dip of the runnel trough and crest were also r rded. Dip of the runnel trough compared with the runnel c t indicated the downstream. An index of roundness was

d sed to note variations in the sharpness of the runnel e s.

Fracture and runnel densities were also determined. T total number of similarly oriented fractures along a w -defined distance were recorded. The dominant fracture o ntations were about 25° NNE, 100° ESE and 140° SE. R el density was similarly determined. The tape measure w laid horizontally along the strike at 1.5 m, 3.0 m and 4 m distances downslope.

2 2. ROCK ANALYSIS

Karren development may be influenced by lithologic v ations. To test this, five specimens were taken from a rnate blocks of the main dip slope and from the other d slopes where runnel features were measured. Chemical d erences were determined by analyzing the purity of s ral rock samples. Specimens from blocks A-B and G-H of t main site were selected as they represented the most d antly separated portions of the slope. A rock sample f n block D-E represented a section with well-developed s ution runnels. Two samples from nearby slopes, where r el measurements were made, were also analyzed. One s e across from the main section was highly fractured, w e another, down the road a short distance, had much moss g th.

A 20 g to 50 g section was sawn from each of the sp imens, cleaned with dilute hydrochloric acid (HCl) and dr d at low temperature (100 ^{o} F) for two days. The se ions were then weighed and dissolved in 9N HCl. The re ltant solutions were filtered and dried. The residual ir lubles enabled determination of the purity of the va ous limestone slopes studied.

2. 3. STATISTICAL ANALYSIS

The relationships existing between the morphometric ch acteristics of karren features were analyzed using co elations and simple linear regressions. A 95 per cent (α =.) confidence interval was applied. Histograms of the av lable data were also plotted for analysis. For example, th most frequent occurrences of Hortonian runnel lengths, wi hs, depths and w/d ratios were determined from these pl s. These analyses were executed with the Minitab co uter package on the Science Vax 8600 system. The raw da and regression analyses are available in Appendix B.

CHAPTER THREE

RESULTS AND DISCUSSION

3.1 INTRODUCTION

This section discusses analyses of the mapping, lithology and solution runnel characteristics.

3.2 MAPPING

The spatial distribution and observable relationships of the karren features on the main site, blocks A-I, are pictorially represented in Figure 3.1. There are distinct belts of dense fracturing with rubble and much less fractured surfaces with lapies wells and gravitomorphic karren. The densely fractured areas are accompanied by large fractures and grikes. Solution runnels are prominent in blocks A-C and D-F. Burned tree stumps, roots and logs along the slope are evidence that this was once a forested area.

3.2.1 FRACTURES

The slope has many fractures which vary in length, width, depth and orientation. Blocks A-D have fractures similar in these characteristics. They range from 0.14 m to 2.98 m in length. Widths were found most frequently to be between 15 cm and 38 cm with depths of 0.5 cm to 93 cm. Block A-B has two of the largest grikes in the section. These are 5.42 m and 7.27 m long respectively, having widths

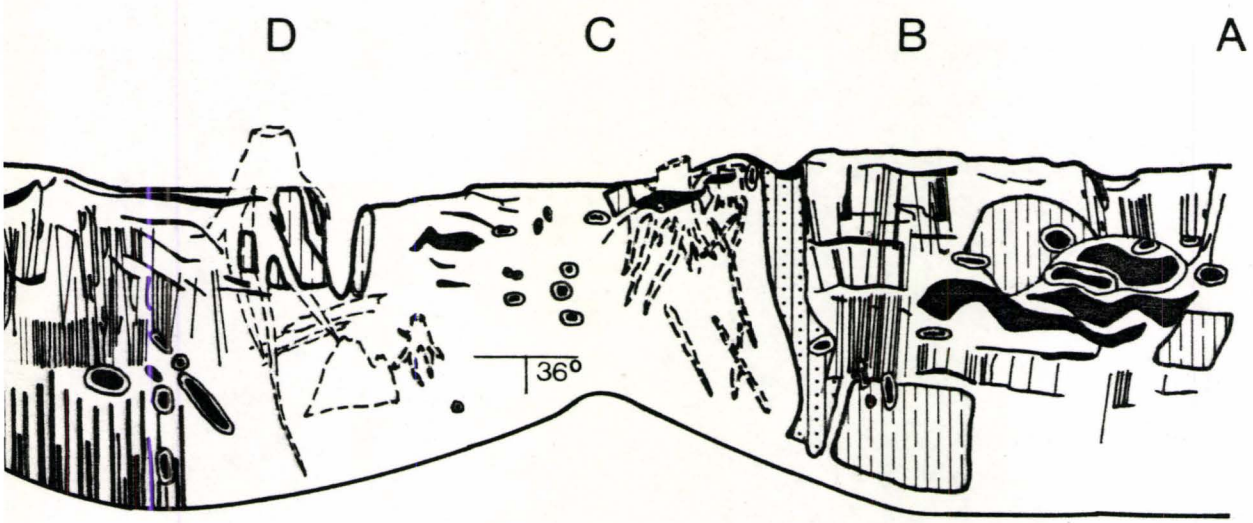

5 metres

5. Kluftkarren (grikes) and fractures

6. Dense fracturing

7. Rubble and dense fracturing

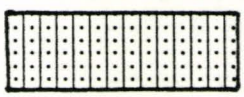

8. Tree stumps, roots and logs

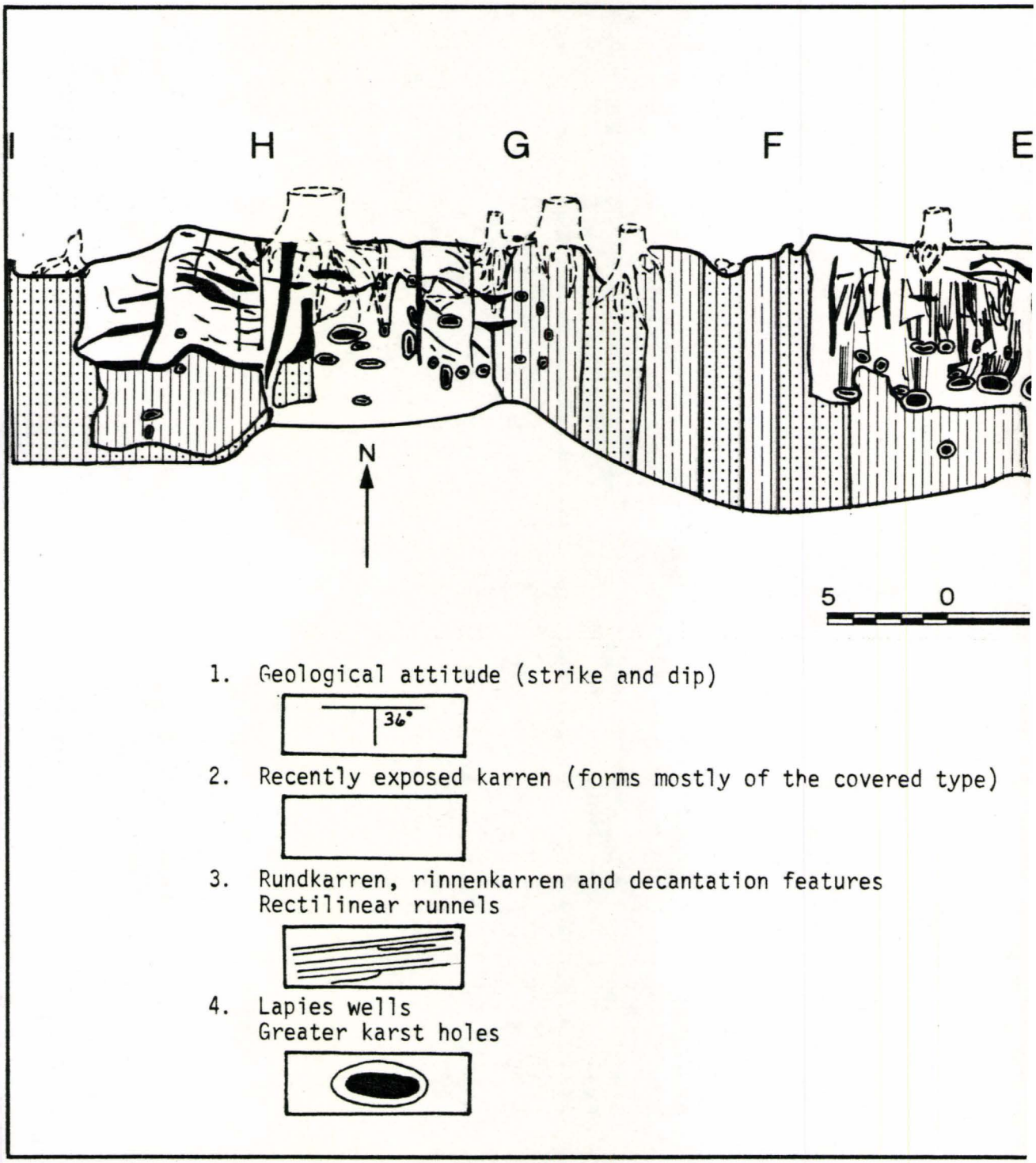

Figure 3.1: A Quatsino Formation dip slope

of about 47 cm and depths of 38 cm. Generally, fractures on this portion of the slope average 1.2 m length, 7.0 cm width and 12 cm depth.

Section D-I, excluding F-G, also have fractures and grikes with comparable characteristics. These features vary from about 0.20 m to 3.94 m. Depths range from 2 cm to 87 cm with corresponding widths of 1.5 cm to 78 cm. On average these fractures are 1.10 m long with widths and depths of 7 cm and 24 cm respectively. Subsections D-E and G-I have many large fractures and grikes. Block H-I, especially, has many grikes of various lengths with widths greater than 15 cm and depths in excess of 30 cm. In general, length and width of fractures are fairly consistent across the slope. Depth, however, seems to increase. Block H-I appears to have the greatest fracture depths. A total of 129 fractures were measured across this 80 metre section. Eighty-two per cent were found to have depth greater than width.

A histogram of fracture length frequencies (Fig. 3.2, in Appendix A) illustrates a logarithmic relationship. This relationship was tested by transferring the data logarithmically to see if a linear relationship resulted. The transformed data was then regressed. Therefore, one may conclude that the fractures on this particular slope are not normally distributed. A significant number of the fractures measured were less than 1.0 m long. The fractures decrease

in length logarithmically such that between 7 and 8 m only one fracture was recorded.

There seem to be no apparent relationships between length versus width or depth all along the slope section. An example of fractures from blocks B-C and H-I tabulated below (in Table 1) illustrate this.

TABLE 1

Length (m)	Width (cm)	Depth (cm)
0.35	6.3	5.0
1.32	9.4	5.8
6.75	19.3	59.5
3.29	28.8	87.3

The dominant fracture orientations observed are 15° to 30° northeast and 135° to 150° northwest. This is illustrated in Figure 3.3 (Appendix A). 37.8 per cent of the fractures measured were orientated between 15° and 30° NE. The majority of the large grikes are also oriented in this direction. Hence, this may reflect the direction of the orogeny. Many large grikes are also orientated at 90° (105° -120°) to these ones. These fractures predominate in blocks B-D, E-F and H-I. Several vertical fractures are also evident in the lower portion of block D-E. Fractures orientated at 135° to 150 NW are dominant in blocks C-D, E-F and G-H. These kluftkarren comprise 17.4 per cent of the total measured.

Fracture densities per metre were greatest for kluftkarren having orientations of 60° to 75° NE. These fractures may be caused by shear stress between the large grikes. Densities of 14 fractures per metre were measured. Orientations of 0° to 30° NE have densities of about 13 fractures per metre. Thus it is apparent from Figure 3.4 (in Appendix A) that fracture density does not vary significantly with orientation. With fracturing as dense as this it is certain that fracture control will dominate the karren type.

Areas of densely fractured and rubbly material are very distinct across this section (Fig.3.5). Specifically the lower portion of the defined slope of E-F and the entire block F-G. The latter section of block E-F and block F-G has a somewhat undulating surface. The ridge areas are densely fractured while in the troughs some of the dense fracturing has become broken. Hence, rubble remains intermixed with the dense fracturing. Subsections B-C and H-I also have large sections of dense fracturing and rubble. Blocks A-D have small isolated areas of dense fracturing.

3.2.2 LAPIES WELLS

Lapies wells are distributed across the whole of the 80 metre dip slope, but they occur most frequently in the less fractured areas (Fig.3.6). They vary only slightly in

Figure 3.5: Densely fractured and rubbly section of the 80 metre dip slope. Fractures are orientated at about 17° NE.

Figure 3.6: Ideal Hortonian rundkarren and a deep lapies well.

size and shape. An average well on this slope has a width of 50 cm, a depth of 80 cm and a downslope length of 54 cm. The features vary in shape from circular to quite elongated. The wells are quite frequently deeper than they are wide. Some wells may be complex, for example, the large well in block A-B, which contains two smaller wells. Lapies wells are aligned in similar directions to the fractures. Orientations of 0^{o} to 30^{o} NE and 135^{o} to 150^{o} NW predominate. No apparent trends in well formation are evident. They occur in association with solution runnels, kluftkarren and even in areas of dense fracturing. These relationships are evident in block A-B.

3.2.3 SOLUTION RUNNELS

Solution runnels are well-developed in only a few sections of this 80 metre dip slope. They are very distinct in block A-B overlapping into B-C, and in blocks D-F. Subsections A-C appear to have many single channel features. Composite forms intermixed with single channels occur frequently in blocks D-F. Most of the runnels have fairly rounded shoulders. Many burned tree stumps and logs on blocks D-F indicate that forest vegetation may have been a contributing factor in the development of solution runnels.

The map provides a visual representation of a Quatsino Formation dip slope. Distinct areas of dense fracturing and rubble are observed. Lapies wells and

solution runnels are associated with the less fractured surfaces. The charred tree stumps on the bare limestone slope indicate a deforested, burned site.

3.3 LITHOLOGY

Lithologic inhomogeneities along the slope might be a factor contributing to the variations in the karren forms. A selection of the hand specimens collected were analysed to determine the solubility of the limestone. The results are recorded in Table 2. The limestone at the relevant field sites ranges from 92 to 96 per cent soluble. Hence, the limestone slopes where karren forms are evident consist of pure limestone. Chemical purity, therefore, should not cause variations in the karren features along the dip slope. Other aspects of lithology were not examined.

3.4 SOLUTION RUNNEL CHARACTERISTICS

Morphometric characteristics of small-scale karren features were carefully measured to provide data for the analysis of significant relationships. The analyses have been concentrated on the morphometric relationships of solution runnels. First, the individual characteristics of width, depth, width/depth (w/d) ratio and length are examined. Second, the relationships of width versus depth, width versus length, depth versus length and the w/d ratio

TABLE 2

Limestone Solubility

Sample	Rock	Filter paper	f.p. & Residue	Residue	% Insolubles
A-B	50.79	4.05	7.06	3.01	5.93
D-E	30.88	4.05	6.18	2.13	6.90
G-H	47.85	3.90	7.41	3.51	7.34
KS_1	32.73	3.89	5.30	1.41	4.31
KS_2	31.88	3.87	6.46	2.59	8.12

% Insoluble

$$\frac{3.01}{50.79} \times 100 = 5.93\%$$

versus length are considered. These relationships are examined for runnel features in aggregate and separated into Hortonian, decantation and composite types. Length is specified as the explanatory variable while width and depth are the dependent variables.

The aggregated runnels range in length from less than 1 m to 8 m (Figure 3.7 to 3.9 in Appendix A). Width and depth fall between 0.0 and 35 cm. The mean length is 2.21 m with the modal length between 1 m and 2 m. The associated width and depth are 6.5 cm and 4.8 cm respectively. Width, depth and length all display unimodality with positive skew. The width curve is only slightly skewed and the distribution remains symmetrical with the mean, median and mode all between 6 to 7 cm. The w/d ratio histogram is very striking. It is a leptokurtic pattern with the mean, median and mode all between 1:1 and 2:1.

The Hortonian runnels have lengths predominantly between 1 m and 3 m (Figure 3.10-3.11). Their widths vary from 3 cm to 35 cm while depths lie between less than 1 cm and 35 cm. The mean length is 2.14 m with width of 8.6 cm and depth of 7.3 cm. Once again, the most frequent w/d ratio is between 1:1 and 2:1. The Hortonian runnels have very distinct histogram patterns. Both width and depth show few variations in frequency for a large range of widths and

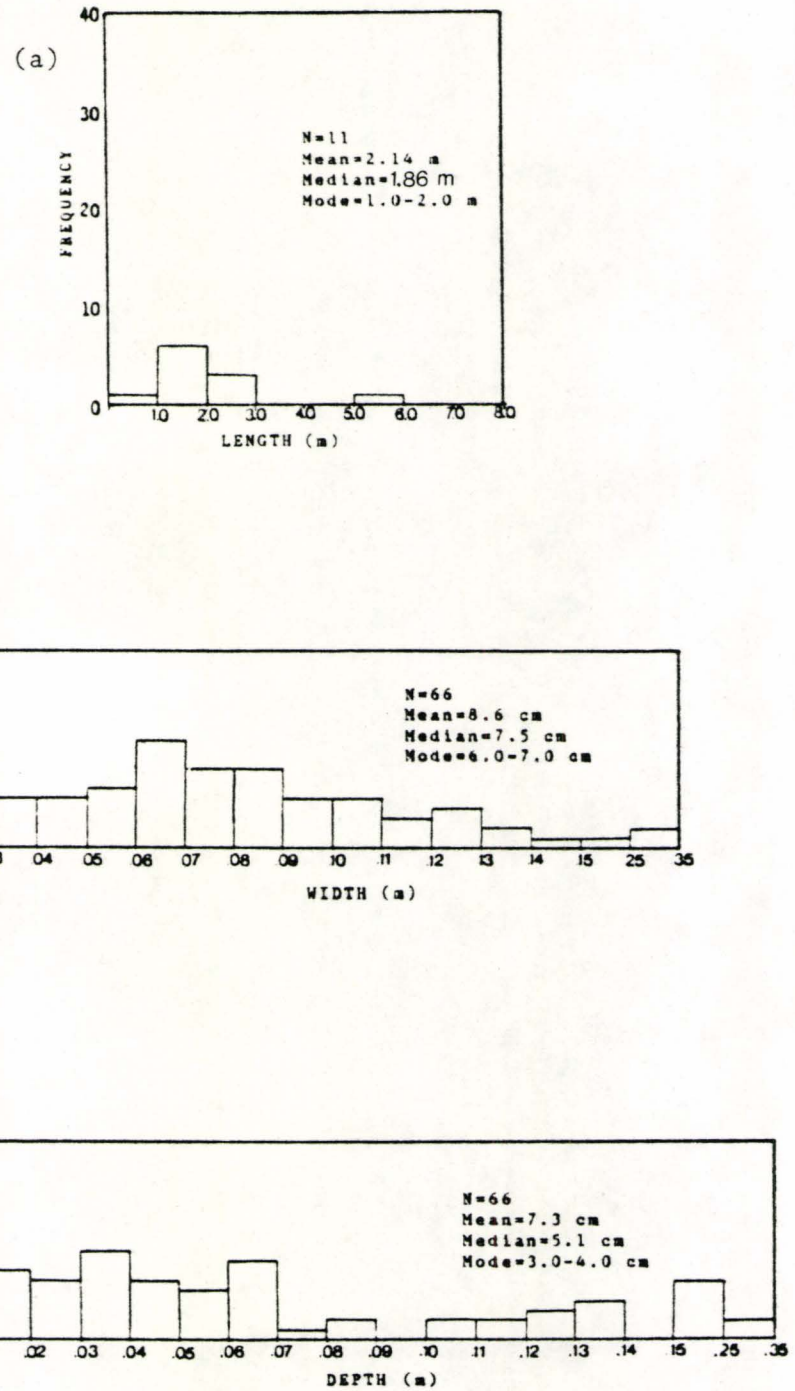

Figure 3.10: Histogram of Hortonian runnel (a) lengths, (b) widths and (c) depths

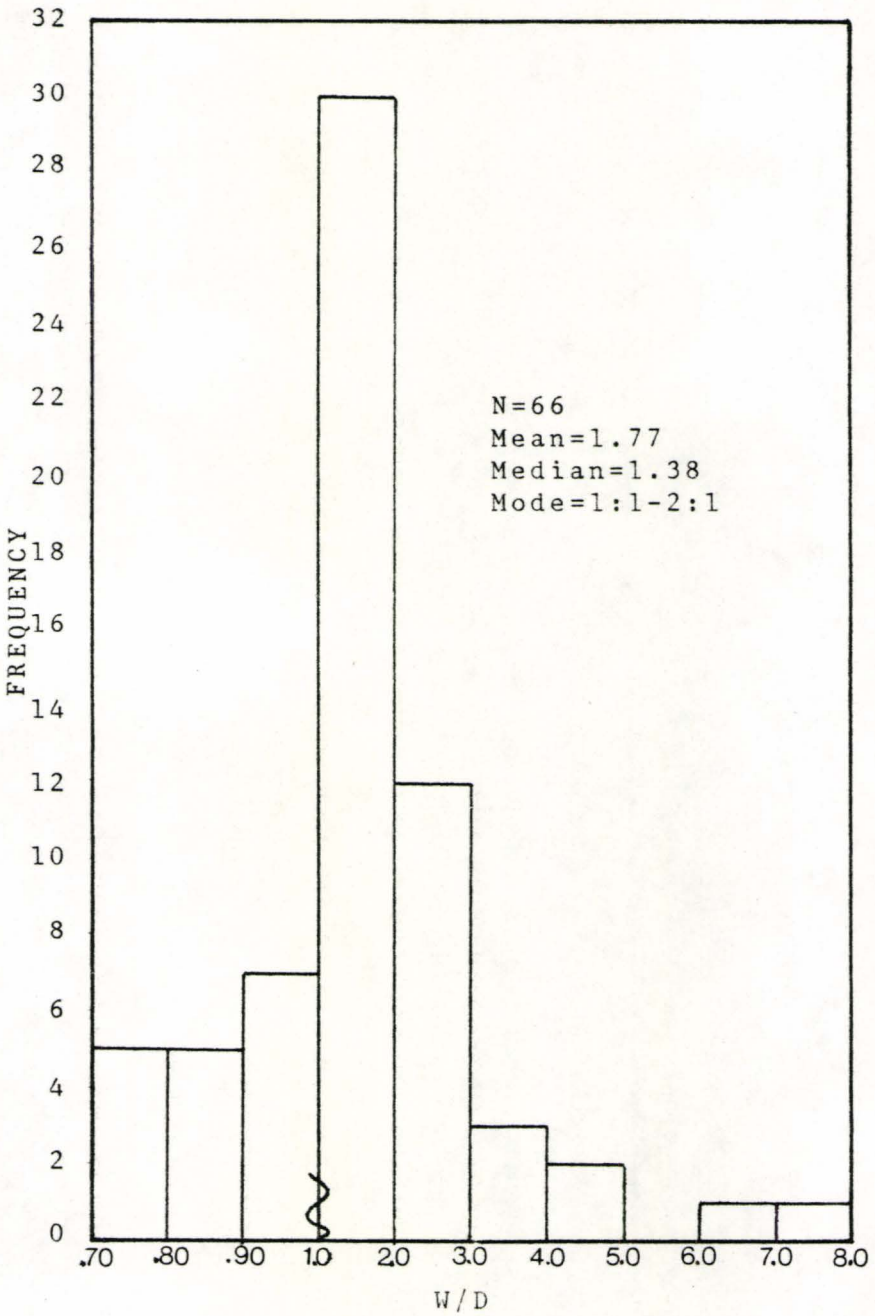

Figure 3.11: Histogram of Hortonian runnel width/depth ratios.

depths. They have platykurtic or flat distribution patterns. The w/d ratio histogram displays the leptokurtic pattern similar to the aggregates.

Decantation runnels also have total lengths ranging between a few cm and 3 m (Figure 3.12 in Appendix A). These runnels have widths varying between 1 cm and 7 cm and depths of less than 1 cm to 5 cm. Decanters were found to have mean lengths of 1.03 m, widths of 4.2 cm and depths of 2.1 cm. Symmetrical to slightly positive skewed histograms predominate for the decantation runnels. Width and depth peak around 4-5 cm and 1-2 cm respectively. The w/d ratios, different from the other categories, are concentrated between 2:1 and 3:1. Length once again shows the slight positive skew.

Composite runnels combine features of Hortonian and decantion features. Composite characteristics were very similar to the aggregates. Total lengths were observed between less than 1 m and 8 m (Figure 3.13-3.15, in Appendix A). Widths varied between 2 cm and 15 cm and depths ranged from 0.0 cm to 25 cm. The mean length of the composite features is 2.34 m with widths of 6.3 cm and depths of 4.5 cm. Widths are concentrated between 6-7 cm and the w/d ratio once again shows the leptokurtic pattern, peaking between 1 and 2. Composite runnels are the most abundant type of solution feature. This means that, for example, the

average Horton runnel cannot extend more than 2 - 3 m before being amalgamated with a decantation form or another Hortonian runnel.

In theory, a perfect minimum friction open channel cross-section is a semicircle. The ratio of width to depth is 2:1. The aggregate, Horton and composite all have a simple leptokurtic form with strong unimodality. Thus, they are close to the semicircular cross-section. Only the decanter is tending to be less regular with a ratio of 3:1.

3.5 STATISTICAL ANALYSIS

The statistical relationships being considered are width versus depth, width versus length, depth versus length and the w/d ratio versus length. These analyses will determine whether the dependent variables vary proportionately with length. These relationships also, are examined for runnel features in aggregrate and separated into Hortonian, decantation and composite forms.

Width and depth of the four runnel categories were correlated to detemine the existence of any associations. The correlation values tended toward 1.0, near perfect positive linear associations. The width to depth relationship of Hortonian runnels showed the most perfect association with a value of 0.944. This value indicated that a linear relationship exits between the width and depth as length increases. Based on the theory of runnel

profiles, width and depth should increase downslope. Decanters had the lowest positive correlation being closer to 0.500. Thus, though a relationship exits between width and depth it is not strongly emphasized.

3.5.1. LINEAR REGRESSION ANALYSIS

The remaining relationships were analyzed using simple linear regressions. The results are recorded in Table 3 of Appendix B. The width versus length relationship was found to be significant for the aggregated runnels and for the Hortonian and composite forms. "Length" refers to distance downslope from the channel head where the measure is being taken. This significance applied for both the student's t-test (variable significance) and for the F-test (regression significance). The correlation of width to length was greatest for the Horton runnels. Similarly, the Horton runnels have the largest amount of variance explained by the regression equation. With a high correlation value and almost 80 per cent of their variance accounted for, Hortonian runnels seem to agree with the theoretical model (Fig. 3.16). The Horton type runnels increase in width as length increases downslope. Aggregate and composite solution runnels have only 25 per cent of their variance explained by the regression equation. They also have low positive correlation values. The composite solution runnels

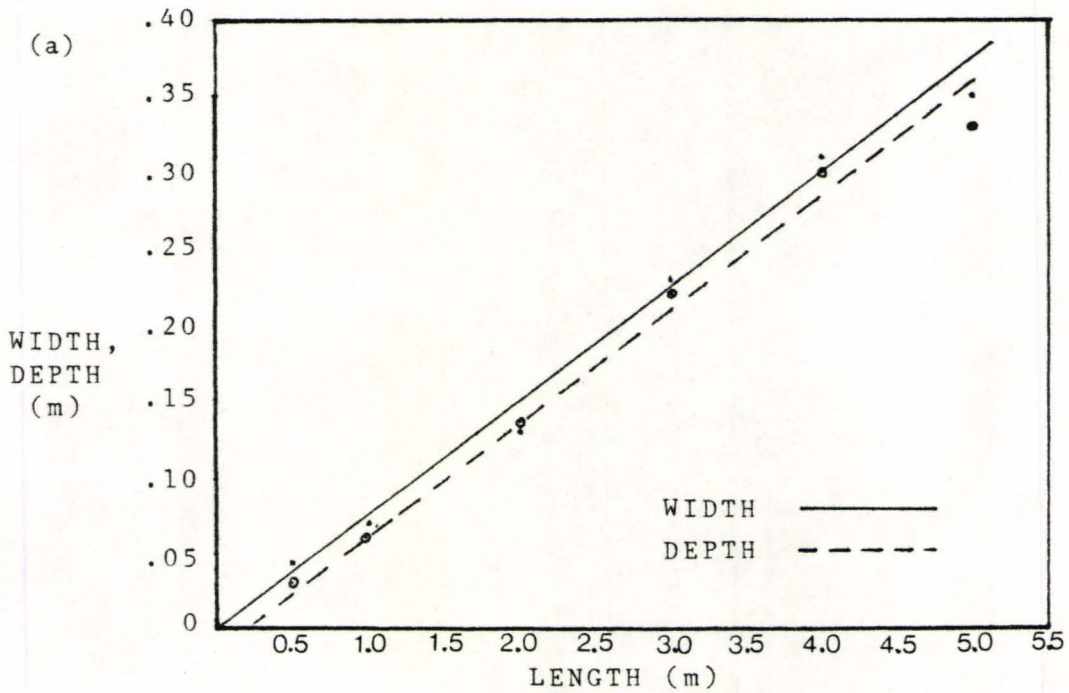

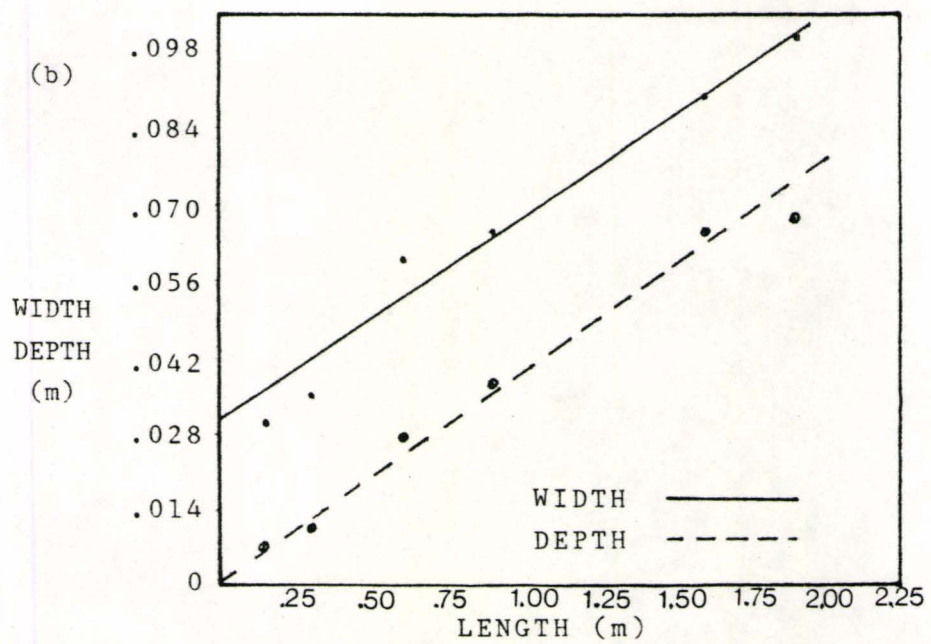

Figure 3.16: Examples of two ideal Hortonian runnels from Vancouver Island. (a) a long runnel, (b) a short runnel.

are not simple runnel features as are the Horton and decantation types. They may deepen disproportionately due to the presence of solvent released from a store. Consequently, a tributary joining the main runnel would increase water flow downslope and cause the channel to deepen (Fig. 1.3). Similarly, a distributary would decrease the flow volume and the runnel would shallow downslope. Decantation features are insignificant with respect to width and length. Theoretically, width should decrease as length increases. The data collected on Vancouver Island does not show this trend clearly. This may be due to the very small sample size. Of all the runnels measured only seven were ideal decantation forms.

The solution runnels illustrated significant relationships between depth and length for the four categories. Horton runnels once more showed the highest positive correlation and were found to have about 71 per cent of their variance explained by the regression equation. These results further confirm that the Hortonian theoretical model applies to the runnel forms. As may be observed in Figure 3.16, width and depth increase simultaneously downslope. The aggregated and composite features once again only had 25 per cent of their variance explained. The depth to length relationship of decantation features tended more strongly in the negative direction than did the width to

length relationship. Though the regression was significant, only about 30 per cent of the variance was explained. This small percentage may once again be explained by the exceedingly small sample size.

The runnel categories all showed significant relationships for the width/depth ratio versus length. All but the decanters which tended somewhat in the positive direction showed a weak negative tendency. The decanters maintained a w/d ratio of 2 to 3 as length increased. Horton's composites and aggregates had w/d ratios concentrated between 1 and 2. However, outliers in the range of 10 to 15 caused the development of the negative tendencies. Figure 3.16 provide examples of ideal Hortonian runnels. Width and depth increase simultaneously with length. Width is somewhat greater than depth in both cases. Fig. 3.16(a) is more than twice the length of (b) yet the relationship remains ideal. These may represent theoretical models of width and depth versus length relationships.

Figure 3.17 (in Appendix A) illustrates the relationships of width and depth versus length for decantation features. Width and depth do decrease with length, but they do not show the simultaneous linear pattern of the Horton's. A tributary junction seems to affect the width more than the depth. Width remains the same between 1.70m and 1.95m while depth continues to shallow. Figure

3.17(b) portrays a more linear relationship though depth tends to decrease more rapidly than width.

Two composite runnels which clearly exhibit the control of Hortonian and decantation characteristics are shown in Figure 3.18. The variabilites of width and depth with length are very distinct in these diagrams. Figure 3.18(a) and (b) are of similar form though (a) is longer. A fracture store at 0.95m causes width and depth to increase for a short distance. It then regains its decanter tendencies. The junction of a tributary at 1.30m increases flow downslope. The runnel, therefore, is controlled by rainfall beyond this point: Hortonian characteristics dominate.

CHAPTER FOUR

CONCLUSIONS

4.1 CONCLUSIONS

The map provides a detailed visual representation of a Quatsino Formation dip slope. The densely fractured areas are associated with rubble, large kluftkarren and fractures. The less fractured surfaces are dominated by lapies wells and gravitomorphic karren.

Fractures are quite variable across this slope. The dominant range of fracture lengths is from less than 1m to 3m. Fractures of less than 1m predominate. These features range in width and depth from a few centimetres to almost a metre. Eighty-two percent of the fractures were found to have depth greater than width. No apparent relationships between length versus width or depth were observed. The dominant fracture orientations are 15^{o} to 30^{o} NE and 135^{o} to 150^{o} NW.

Lapies wells occur along the entire dip slope, but they are best developed in the less fractured areas. An average well on this slope has a width of 50cm, a depth of 80cm and a downslope length of 54cm. These features may be circular or elongated in shape and are frequently quite deep. Many were found to be greater than 1m deep and one had a depth of 3m.

Solution runnels are well-developed in only a few sections of this 80 metre slope. Many of these runnels were measured morphometically so that the presence of significant relationships could be determined. The runnel forms were examined in aggregate and separated into Hortonian, decantation and composite types. Composites were the most abundant. The aggregated data and composite runnels had lengths near 2 m ranging from less than 1m to 8m and widths and depths around 6.6cm and 4.5cm respectively were observed. The Hortonian type forms have lengths ranging between 1.0 m and 3.0 m. The mean widths and depths were 8.6 cm and 7.3 cm respectively. Very little variation in either was evident over a large range of values. Decantation features also have lengths of a few cm to 3.0 m. Typically, on the Quatsino Formation limestones decanters had lengths of 1.0 m, widths of 4.2 cm and were 2.1 cm deep.

Simple Hortonian and decantation runnels are not very common. Usually they amalgamate downslope (typically at about 3m from channel head) to form a composite runnel. Thus the controls on development are multiplied and the form is no longer a simple channel. Instead flow may increase rapidly or a store may intervene to modify the form. Also, the leptokurtic patterns of the Horton, composite and aggregate w/d ratios are quite striking. The common 1:1 to 2:1 ratio indicates a U-shaped or semicircular cross-

section. The decanter tends to be less regular with a 3:1 ratio.

The histograms and regressions reveal that runnel morphologies are well ordered. Hydraulic and hydrochemical mechanisms operate and change downslope as hypothesized to produce Hortonian features which become wider and deeper (in regular proportion)downslope. In contrast decantation rills show the opposite trend and tend to extinguish downslope as expected, although this pattern is not quite so clearly expressed. The development of decantation sites in Horton runnels modify the form. Terminations at lapies wells or the base of the slope all serve to limit the extension of the runnel.

4.2 FURTHER RESEARCH

4.2.1 MAPPING TECHNIQUES

The study of small-scale solutional features is fundamental to the understanding of various aspects of karstic erosion (Sauro,1975). Many publications have adequately described simple, single karren forms and interpreted their origin. Difficulties arise however, when many features are developing as a complex group. The various forms are in different stages of development and they may be difficult to identify. Sauro (1975) felt that geomorphological mapping of a karstic area would overcome

the difficulties of general descriptions. This study provides a map of a Quatsino Formation dip slope. The data available from this research may be used to interpret the genesis of these features and the surrounding environment.

4.2.2 KARREN

Similar studies of karren features should be done in different climates and on different lithologies. Much research is required to elucidate the details of process. Smaller solution features have not been widely examined. A consensus must be attained as to research methods. For purposes of comparison, it is very important that the features of different studies all be measured along the same guidelines. The characteristics of the feature must be carefully defined. Then a useful classification can be devised.

4.2.3 PALEOECOLOGY

Karren may also be important for paleoecological reasons. For example, the area studied on Vancouver Island may be used as a model for older areas. This area was deforested in 1970. Many of the existing forms could not have developed to their present state in 16 years. Hence, they must have developed beneath a cover, as we know they have. This model could be applied to, for example, Hatton Roof in England. The narrow, round-edged runnels here are

very similar to those on Vancouver Island. Thus they are probably also rundkarren which have been modified since emergence from beneath a cover. They now resemble very closely spaced and overdeepened rinnenkarren (Sweeting, 1973). The degree of sharpening may be used as a measure of the time since exposure.

REFERENCES

Beck, B.F. and Cram, C. 1977. On the occurrence and origin of karren on granodiorite in Puerto Rico. Proc. 7th. Int. Spel. Cong., Sheffield, England: 28-31

Bogli, A.F. 1960. Kalklosung and Karren Bildung. Z. Geomorph., Supp. 2, 4-21

Bogli, A.F. 1980. Karst Hydrology and Physical Speleology. Berlin: Springer - Verlag, 284 pp.

Ford, D.C. and Lundberg, J. (in press)

Jennings, J.N. 1985. Karst Geomorphology. New York: Basil Blackwell, Ltd., 293 pp.

Jones, R.I. 1965. Aspects of the biological weathering of limestone pavements. Proc. of the Geologist's Association, 76, 421-34

Lundberg, J. (personal communication)

Mills, W.R.P. 1981. Karst development and groundwater flow in the Quatsino Fm. northern Vancouver Island. M.Sc. Thesis, McMaster University. 170 pp.

National Atlas of Canada. Energy, Mines and Resources Canada, 1974.

Regional District of Mount Waddington Composite Road Map of North Vancouver Island. 1979.

Sauro, U. 1975. Karst Processes and Relevant Landforms. Proc. of the Int. Symp. on standardization of field research., Ljubljana: 189-199.

Stephan, Brenda, Ann, 1987. The Littoral Karren of Neroutsos Inlet, Northern Vancouver Island. Hons. B.A. Thesis. Unpublished.

Sweeting, M.M. 1973. Karst Landforms. London (Macmillan):362pp.

Tozer, E.T. 1967. A standard for Triassic time. Geol. Surv. Can. Bull., 156

Trudgill, S.T. 1976e. Limestone erosion under soil. In: Panos, V. (Ed.) Proc. 6th Int. Cong. of Spel. II. Ba, 409-22. Academia/Prague

Trudgill, S.T. 1985. Limestone Geomorphology. Longman, London and New York, 194 pp.

APPENDIX A

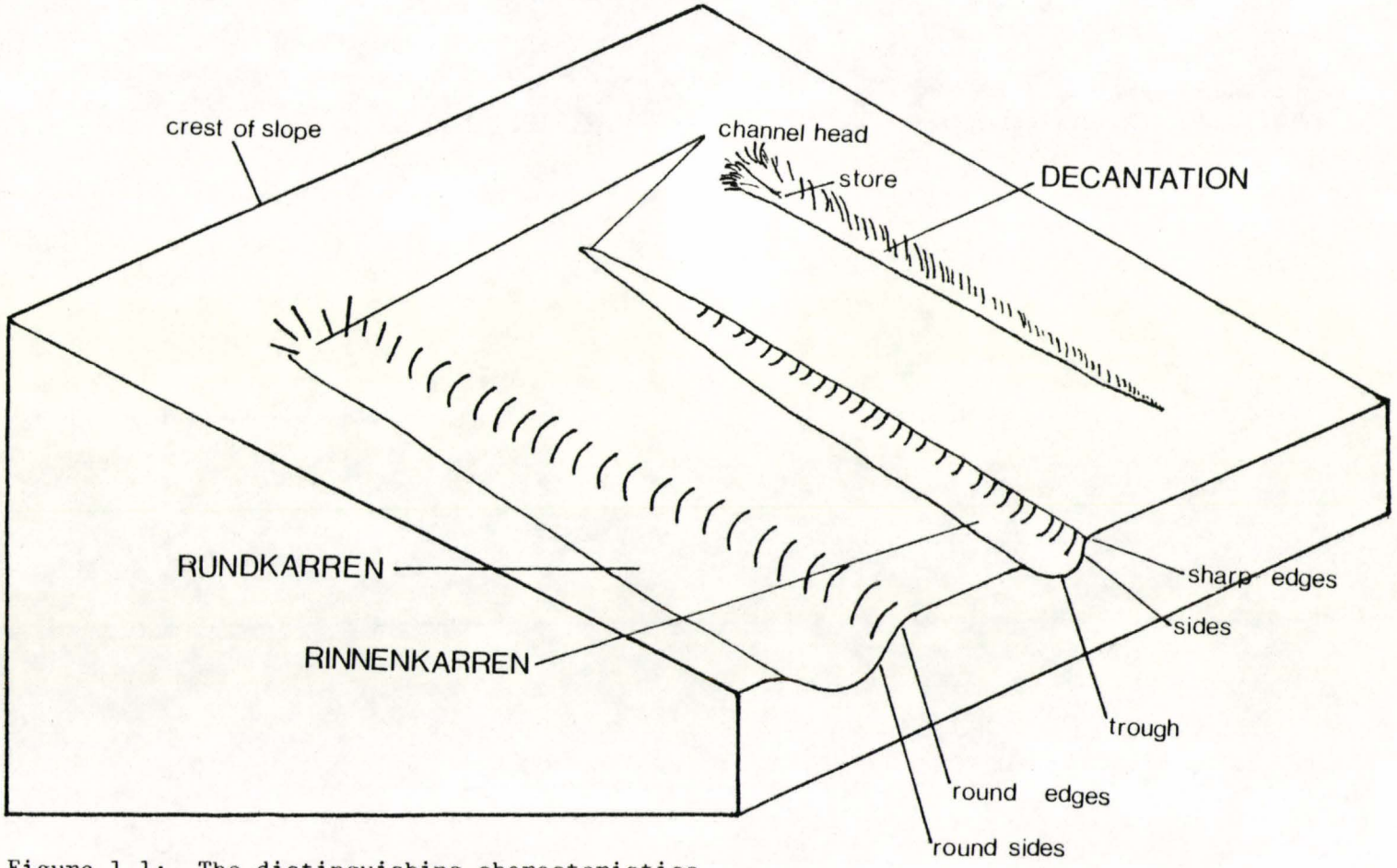

Figure 1.1: The distinguishing characteristics of Rundkarren, Rinnenkarren and Decantation forms.

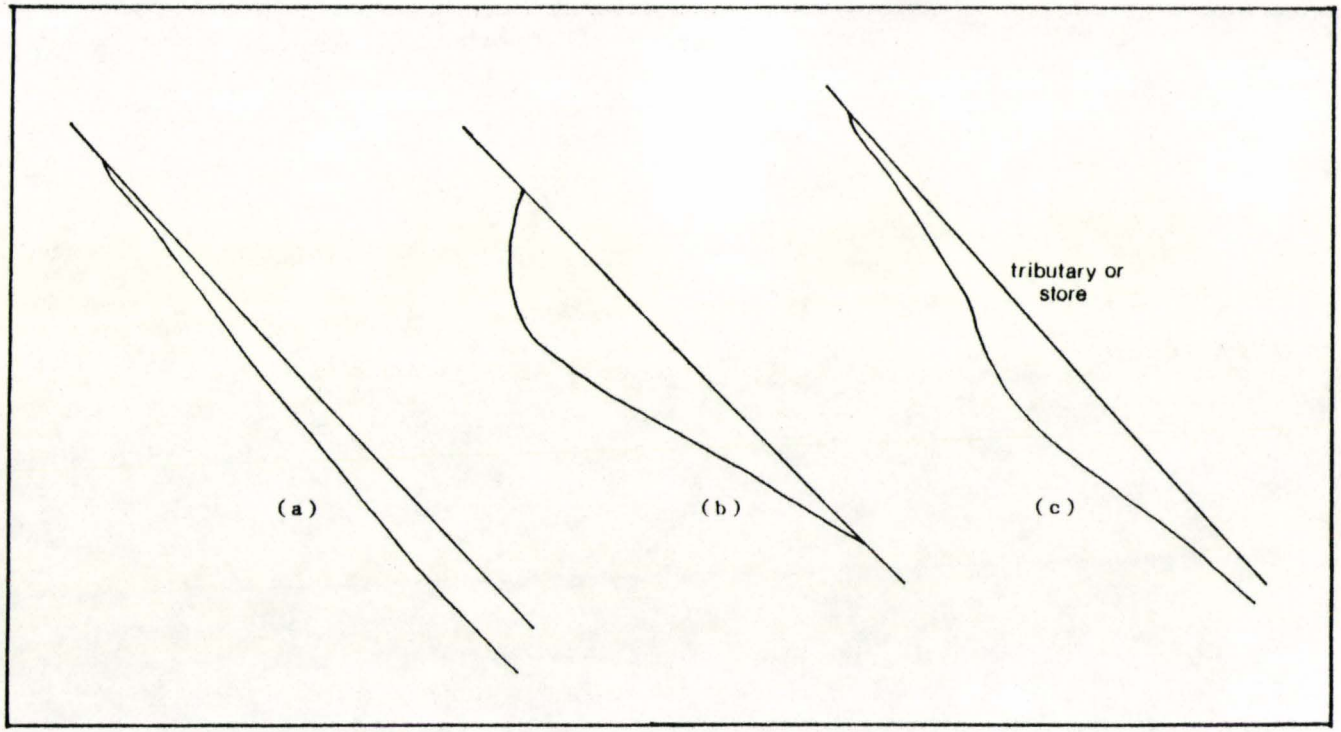

Figure 1.4: Theoretical profiles of the different types of gravitomorphic rills: (a) Horton, (b) Decantation, (c) Composite.

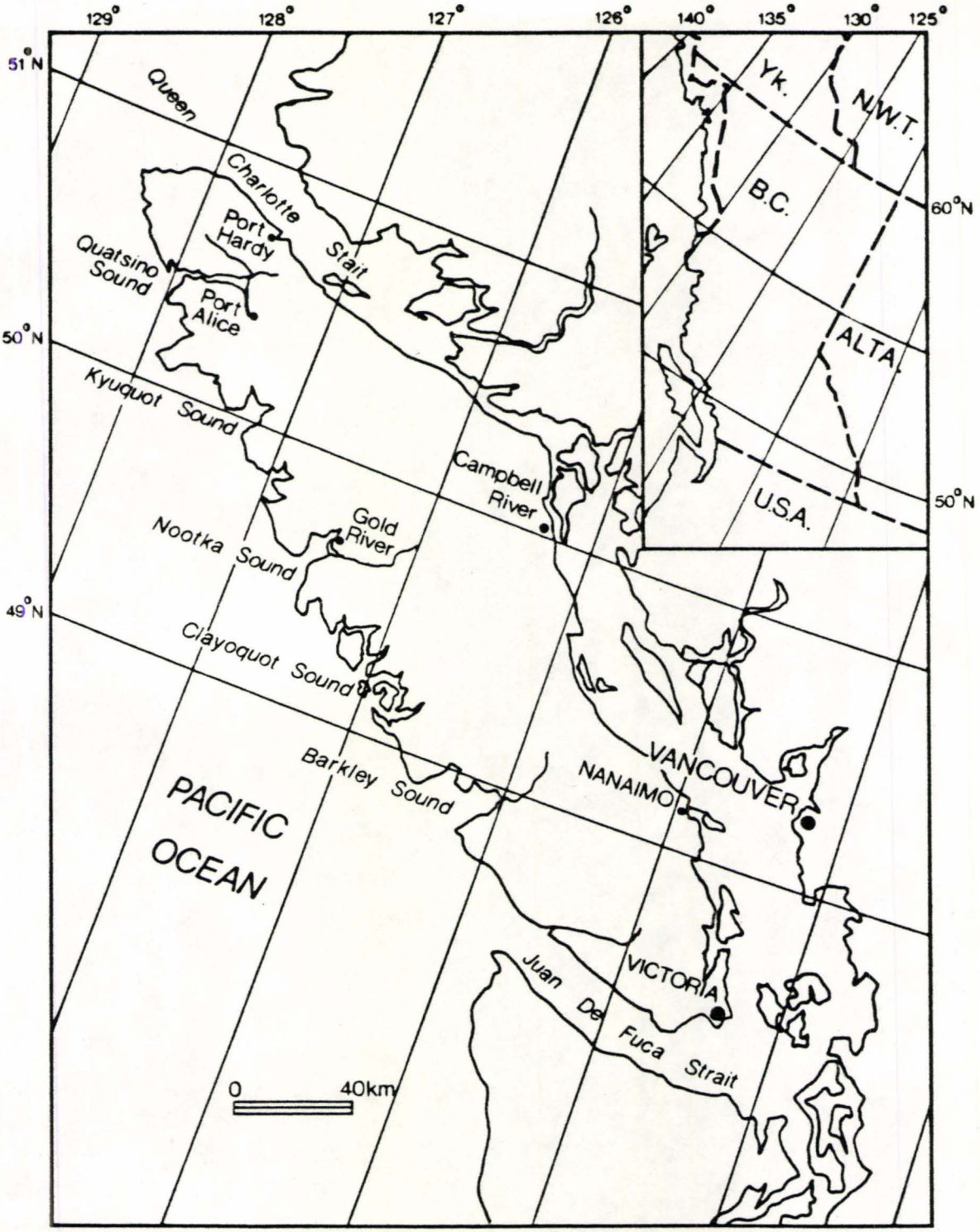

Figure 2.1: Study Site: Northern Vancouver Island (Stephan, 1987)

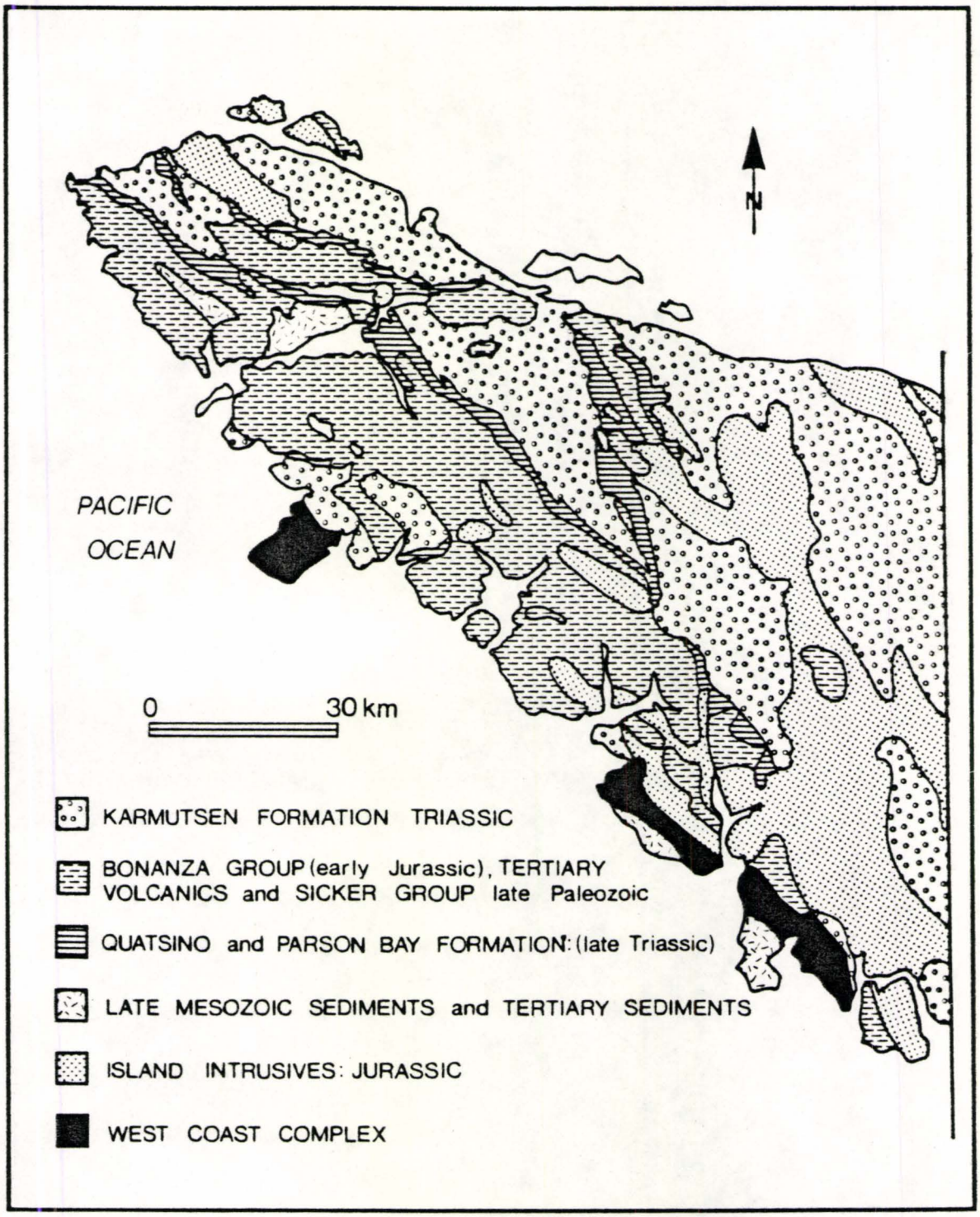

Figure 2.3: Geology of Northern Vancouver Island (Stephan, 1987)

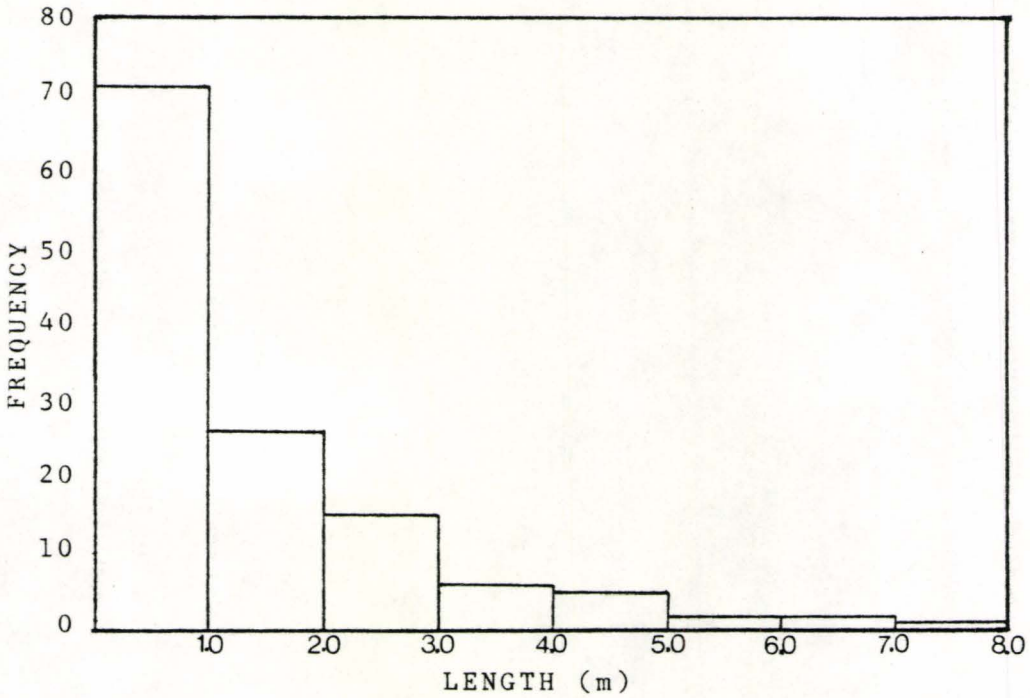

Figure 3.2: Histogram of fracture length frequencies.

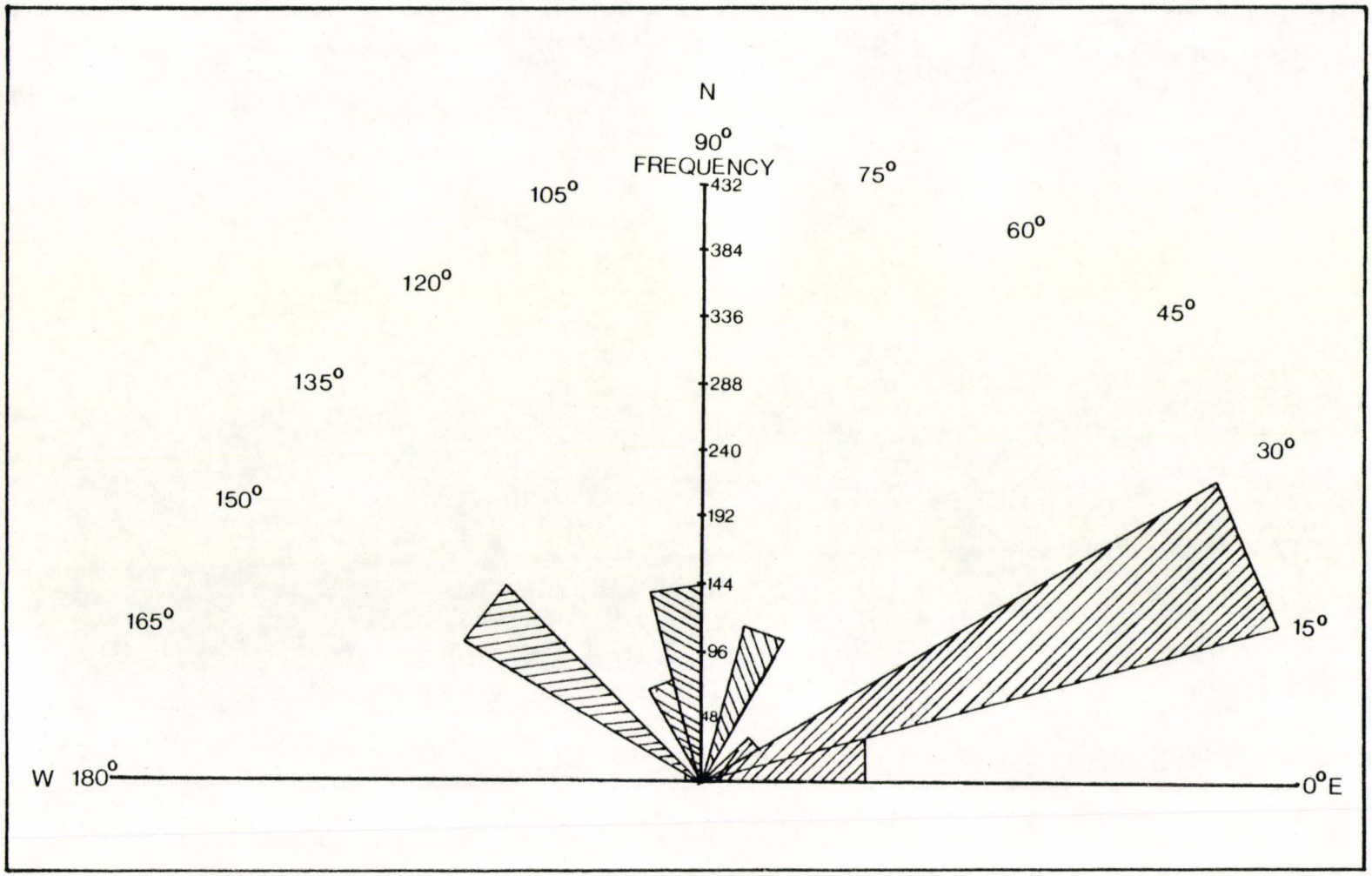

Figure 3.3: Directional rosette of fractures.

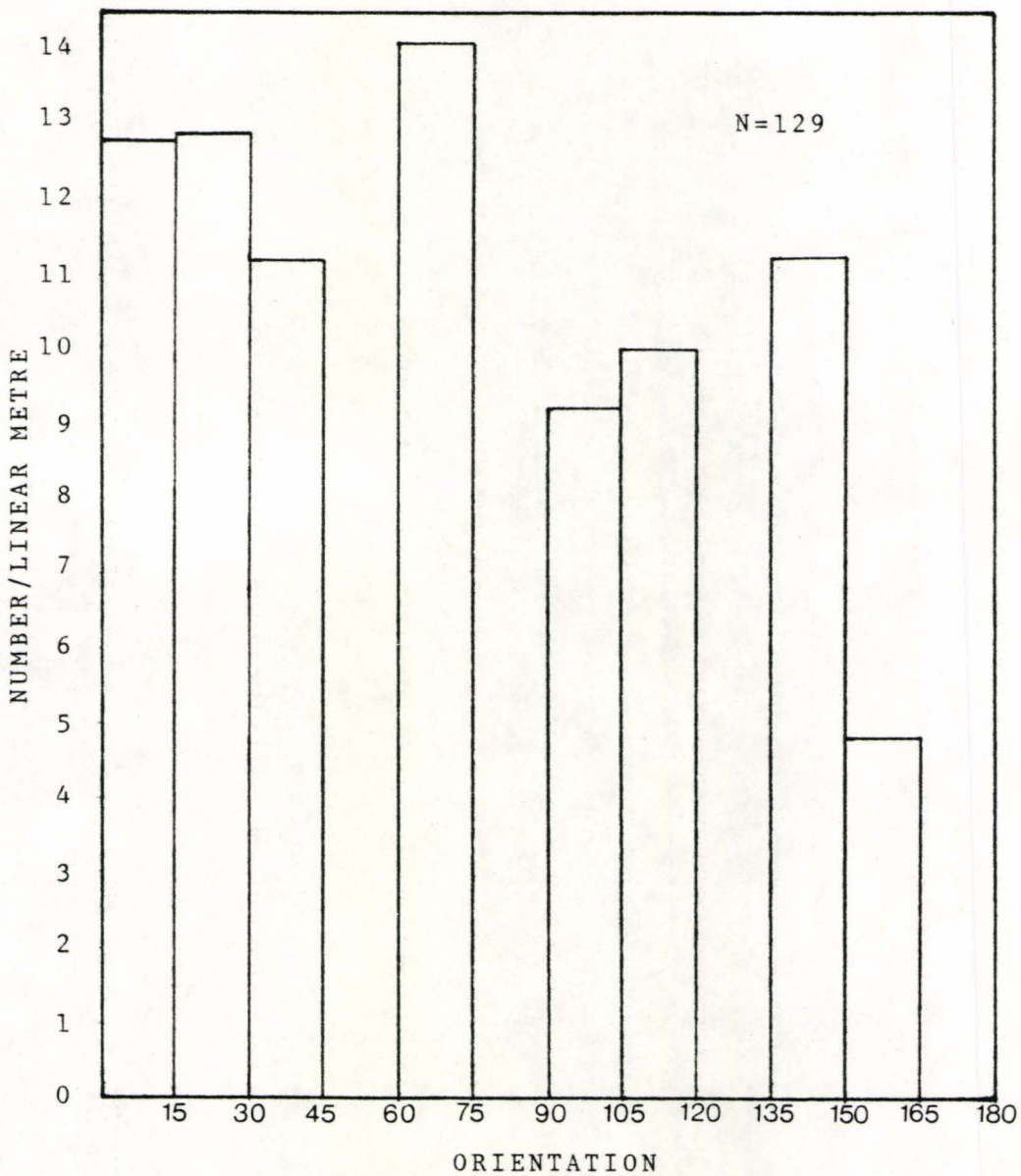

Figure 3.4: Density of fractures per linear metre with respect to orientation.

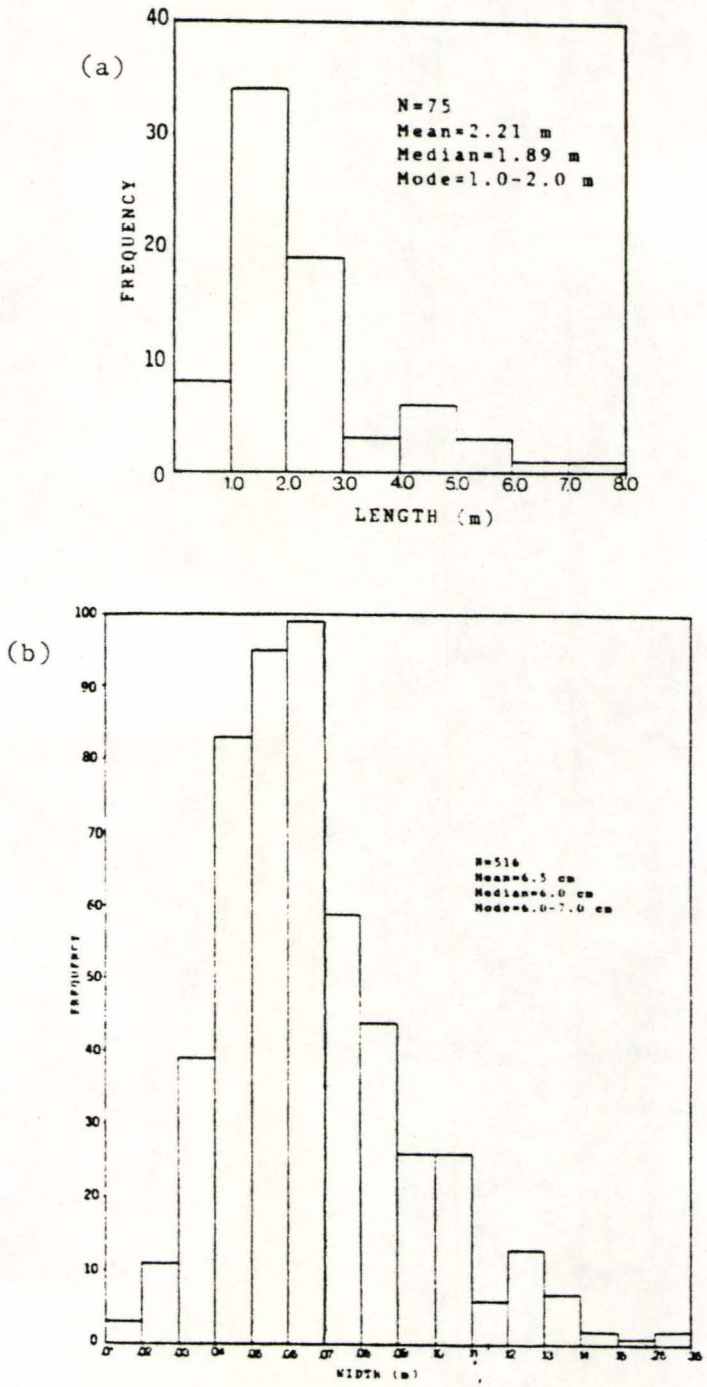

Figure 3.7: Histogram of aggregated runnel (a) lengths and (b) widths

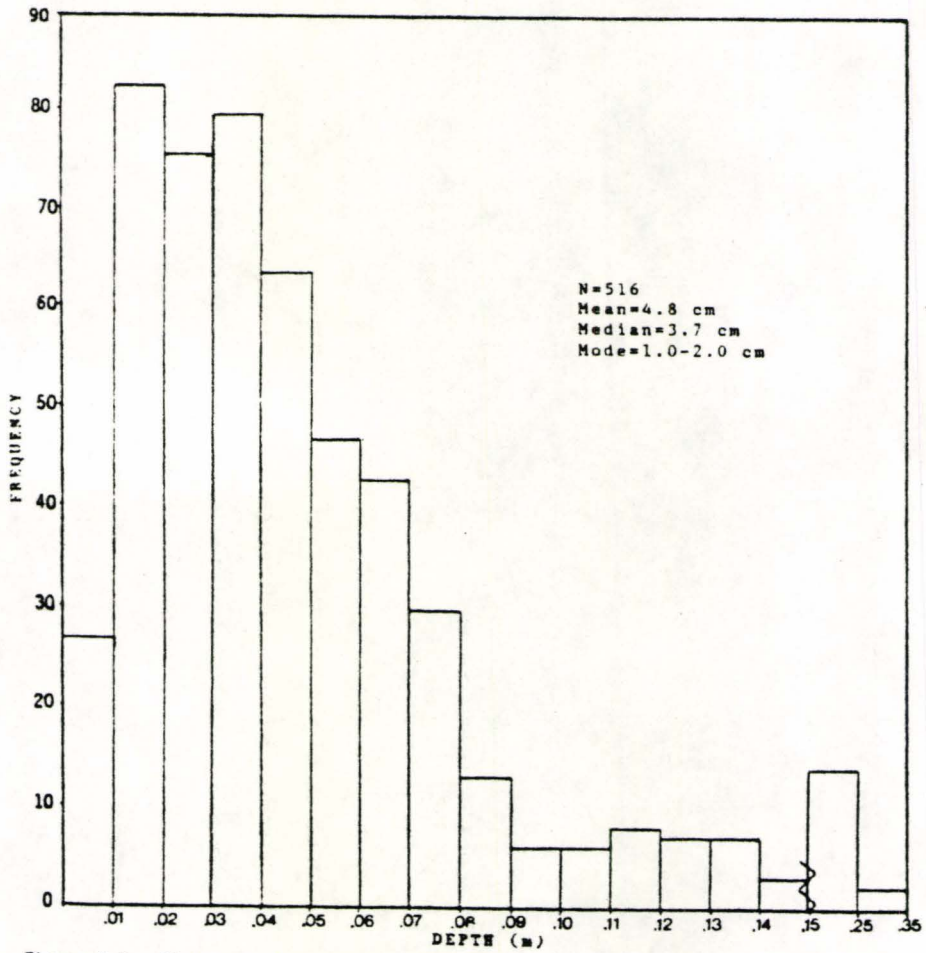

Figure 3.8: Histogram of aggregated runnel depths.

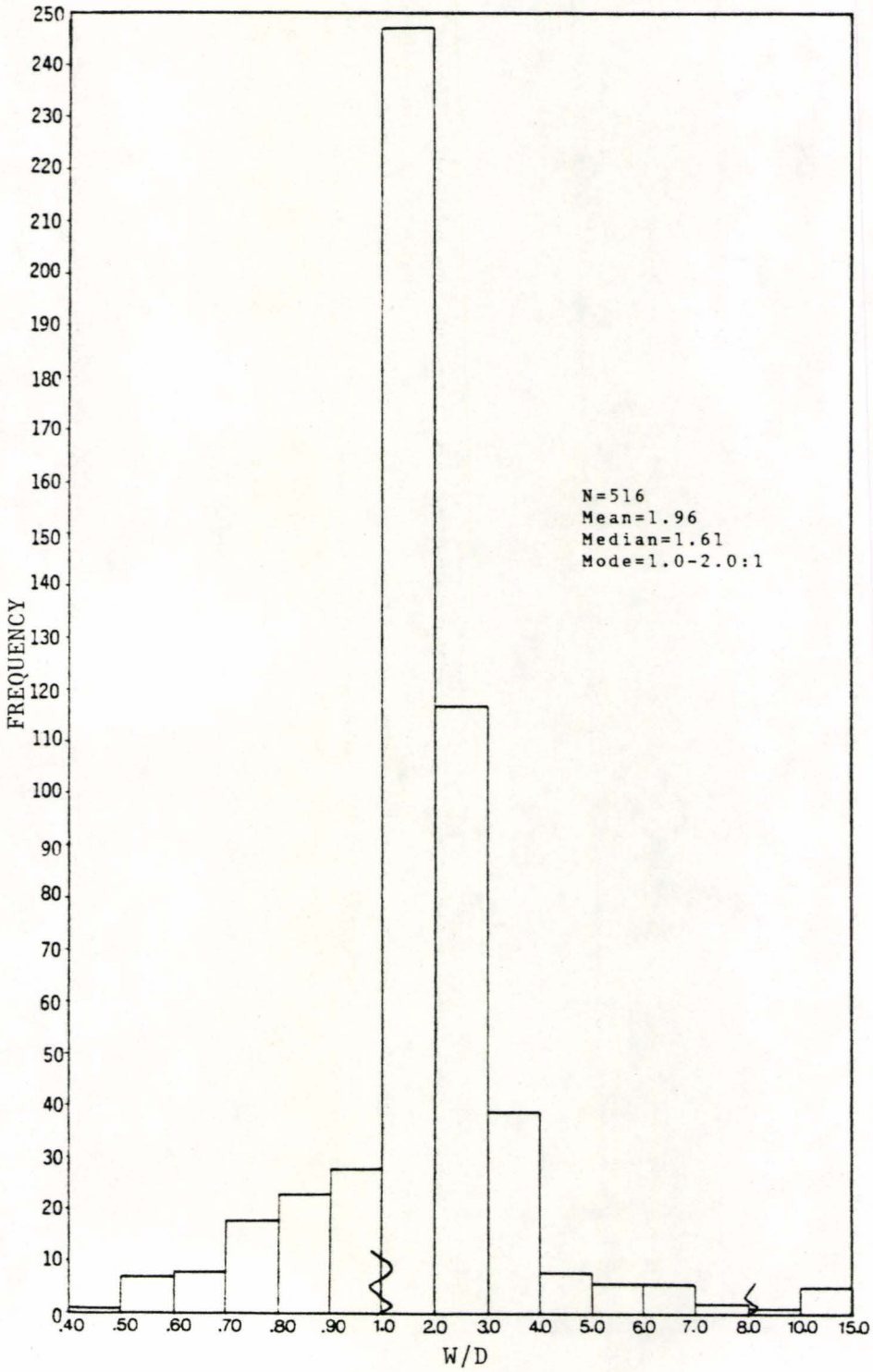

Figure 3.9: Histogram of aggregated runnel w/d ratios.

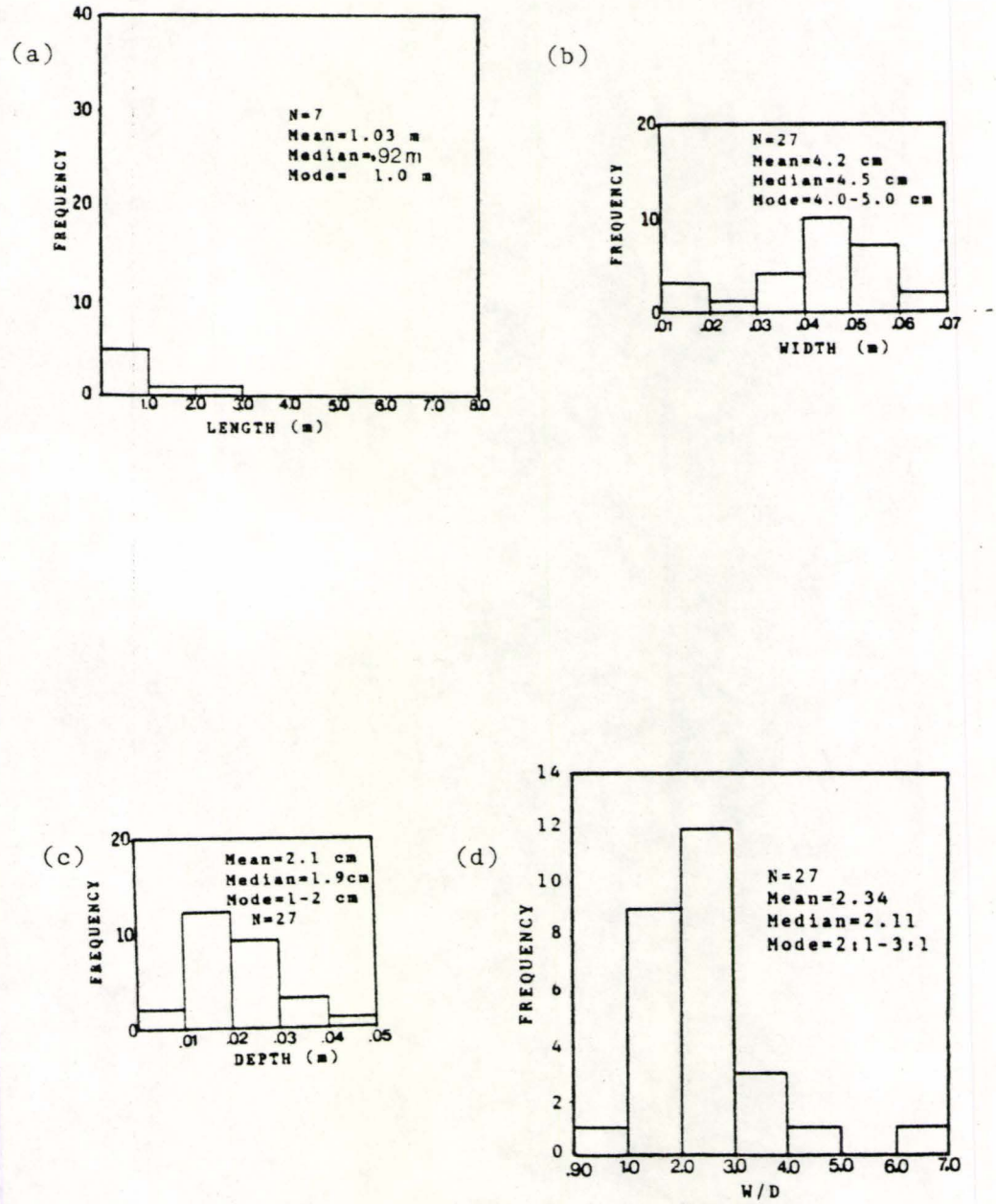

Figure 3.12: Histograms of decantation runnel (a) lengths, (b) widths, (c) depths and (d) w/d ratios

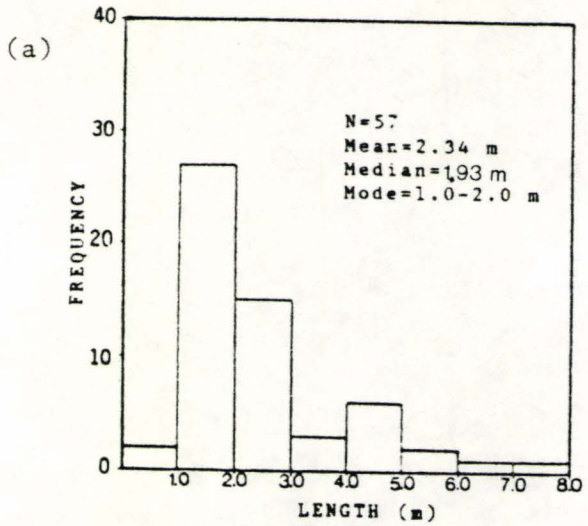

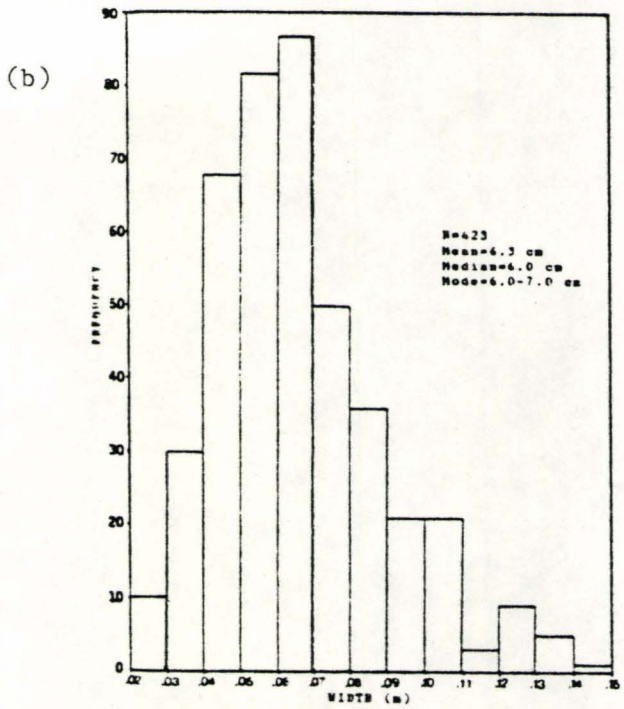

Figure 3.13: Histogram of composite runnel (a) lengths and (b) widths

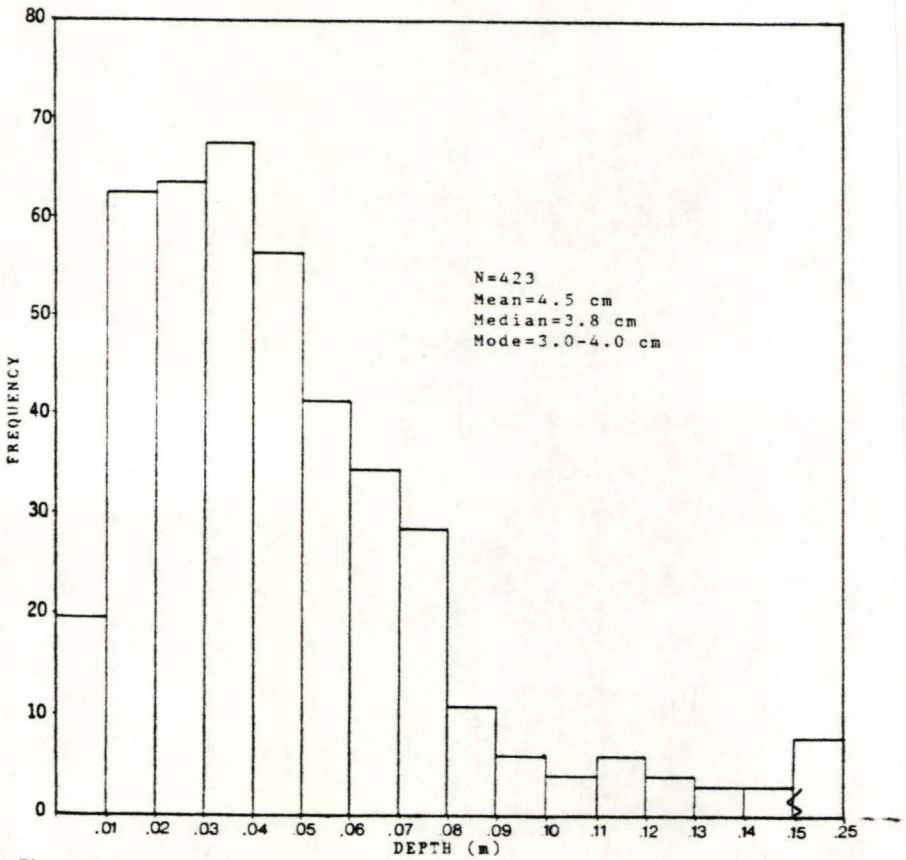

Figure 3.14: Histogram of composite runnel depths.

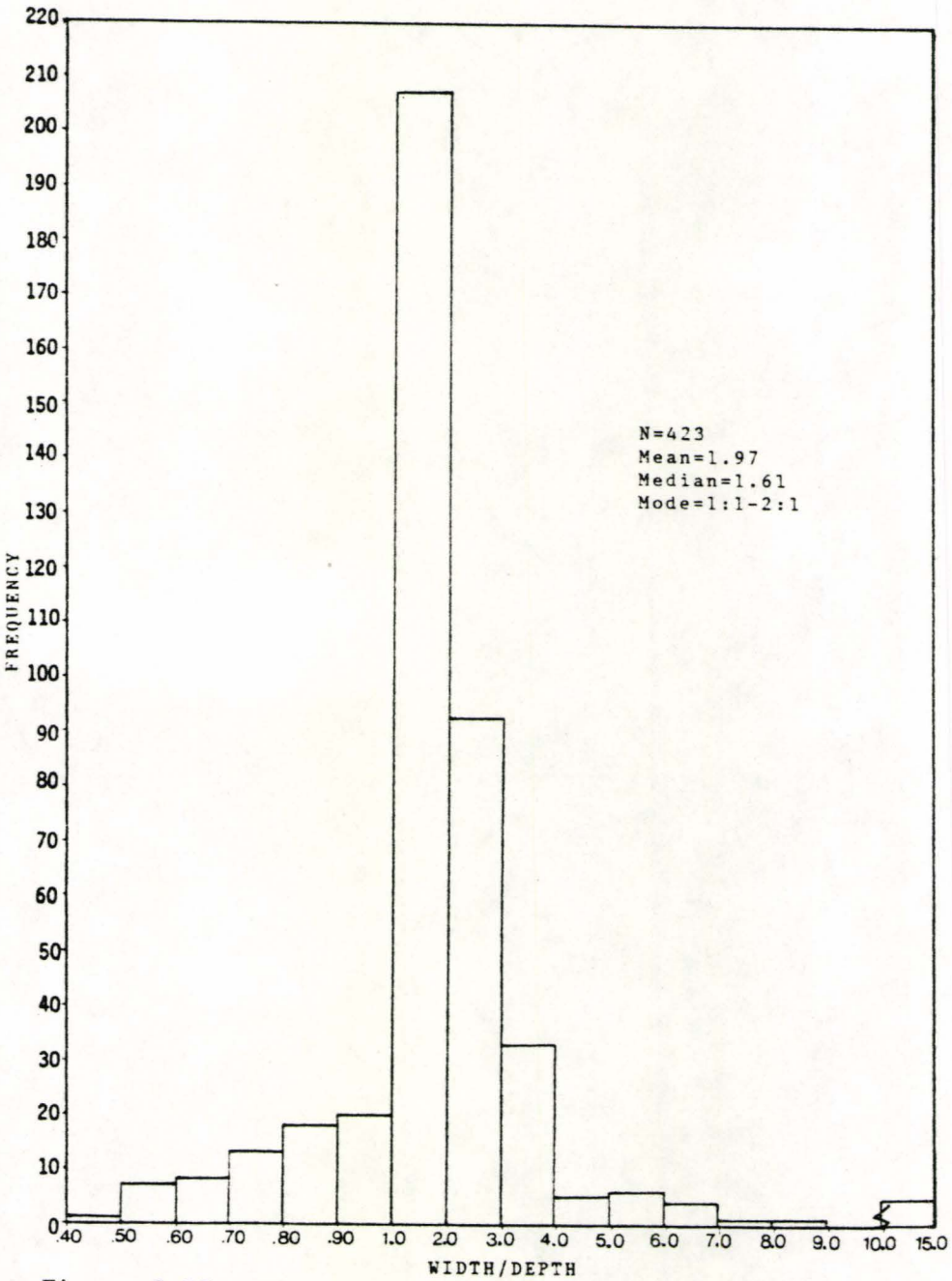

Figure 3.15: Histogram of composite runnel w/d ratios

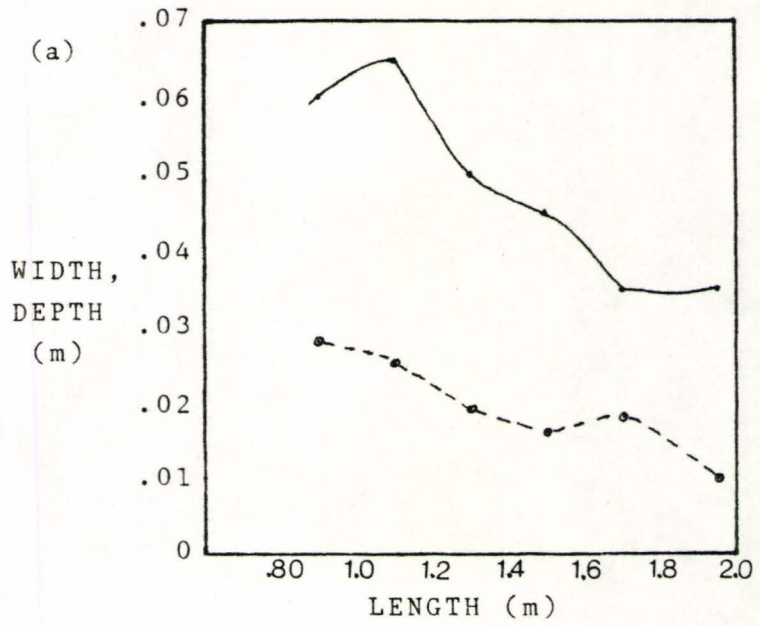

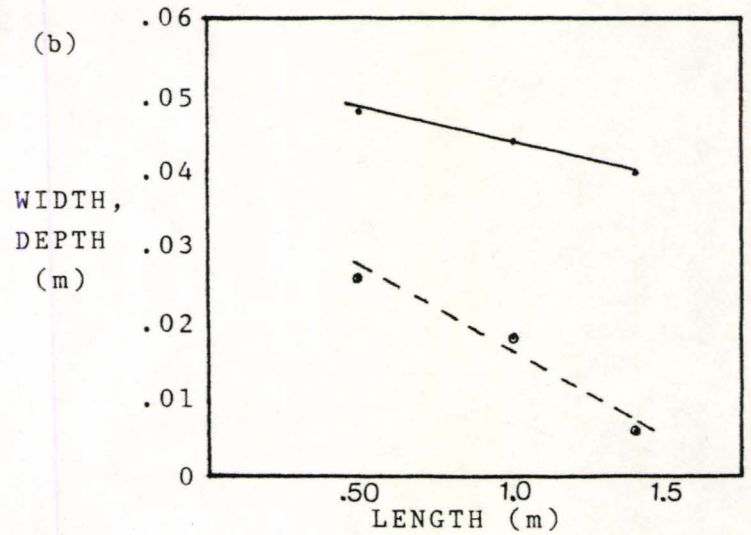

Figure 3.17: Width, depth versus length relationships for two individual decantation runnels, (a) and (b), observed on Vancouver Island.

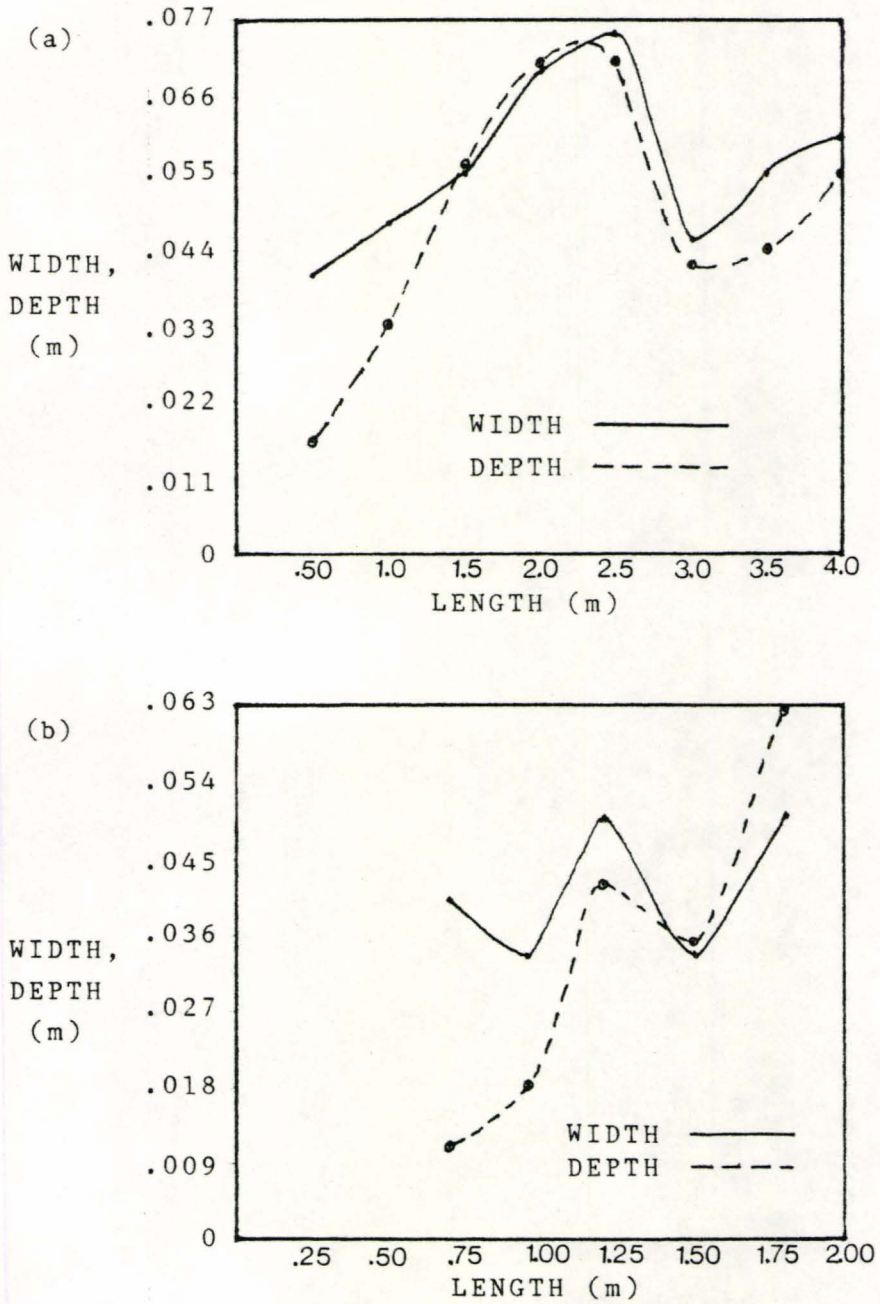

Figure 3.18: Width, depth versus length relationships for two individual composite runnels (a) and (b), observed on Vancouver Island.

APPENDIX B

TABLE 3

LINEAR REGRESSION ANALYSES

1. Relationships of Runnel Width vs. Depth

	Correlation
Aggregate	.830
Composite	.722
Horton	.944
Decanter	.614

2. Relationships of Runnel Width vs. Length

	Correlation	R^2	Significance
Aggregate	.490	23.8%	Yes
Composite	.486	23.5%	Yes
Horton	.890	78.9%	Yes
Decanter	-.131	0.0%	No

3. Relationships of Runnel Depth vs. Length

	Correlation	R^2	Significance
Aggregate	.504	25.3%	Yes
Composite	.501	24.9%	Yes
Horton	.844	70.7%	Yes
Decanter	-.574	30.2%	Yes

4. Relationships of Runnel W/D Ratio vs. Length

	Correlation	R^2	Significance
Aggregate	-.215	4.4%	Yes
Composite	-.207	4.0%	Yes
Horton	-.441	18.2%	Yes
Decanter	.531	25.3%	Yes

(a)

```
MTB > CORR C235-C238

                 C235 (W)    C236 (D)    C237 (L)
C236             0.830
C237             0.490       0.504
C238            -0.297      -0.499      -0.215
```

(b)

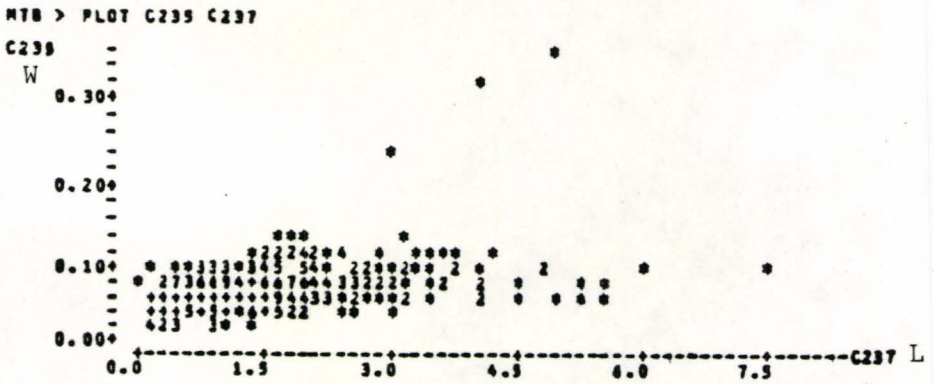


```
MTB > REGR C235 1 C237

The regression equation is
C235 = 0.0465 + 0.0134 C237

Predictor       Coef          Stdev       t-ratio
Constant     0.046466       0.001824         25.48
C237         0.013633       0.001070         12.74

s = 0.02598     R-sq = 24.0%     R-sq(adj) = 23.8%

Analysis of Variance

SOURCE          DF          SS          MS
Regression       1     0.10948     0.10948
Error          914     0.34685     0.00067
Total          915     0.45633
```

Figure 3.19: Correlation (a) and regression analyses of (b) width, (c) depth and (d) w/d ratios versus length for aggregated runnels

(c)

```
MTB > PLOT C236 C237

C236
 D
0.30+
0.20+
0.10+
0.00+
      +---------+---------+---------+---------+---------+---------+-------C237  L
      0.0       1.5       3.0       4.5       6.0       7.5
```

```
MTB > REGR C236 1 C237

The regression equation is
C236 = 0.0232 + 0.0184 C237

Predictor       Coef          Stdev       t-ratio
Constant     0.023161       0.002373          9.76
C237         0.018427       0.001393         13.23

s = 0.03380     R-sq = 25.4%     R-sq(adj) = 25.3%

Analysis of Variance

SOURCE        DF          SS          MS
Regression     1      0.20001     0.20001
Error        514      0.58733     0.00114
Total        515      0.78734
```

(d)

```
MTB > PLOT C238 C237

C238
 W/D
15.0+
10.0+
 5.0+
 0.0+
      +---------+---------+---------+---------+---------+---------+-------C237  L
      0.0       1.5       3.0       4.5       6.0       7.5
 M* = 1
```

```
MTB > REGR C238 1 C237

The regression equation is
C238 = 2.36 - 0.299 C237

515 cases used 1 cases contain missing values

Predictor       Coef          Stdev       t-ratio
Constant      2.3598         0.1025         23.03
C237        -0.29925        0.06007         -4.98

s = 1.457       R-sq = 4.6%      R-sq(adj) = 4.4%

Analysis of Variance

SOURCE        DF          SS          MS
Regression     1       52.656      52.656
Error        513     1088.511       2.122
Total        514     1141.166
```

MTB > CORR C258-C261

(a)

	W C258	D C259	L C260
C259	0.722		
C260	0.486	0.501	
C261	-0.299	-0.537	-0.207

MTB > PLOT C258 C260

(b)

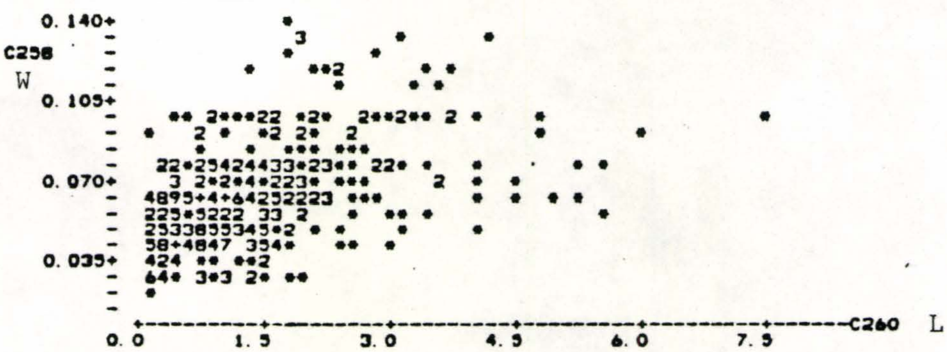

MTB > REGR C258 1 C260

The regression equation is
C258 = 0.0491 + 0.00983 C260

Predictor	Coef	Stdev	t-ratio
Constant	0.049071	0.001528	32.11
C260	0.0098345	0.0008612	11.42

s = 0.01962   R-sq = 23.6%   R-sq(adj) = 23.5%

Analysis of Variance

SOURCE	DF	SS	MS
Regression	1	0.050220	0.050220
Error	421	0.162143	0.000385
Total	422	0.212363	

Figure 3.20: Correlation (a) and regression analyses of (b) width, (c) depth and (d) w/d ratios versus length for composite runnels

MTB > PLOT C259 C260

(c)

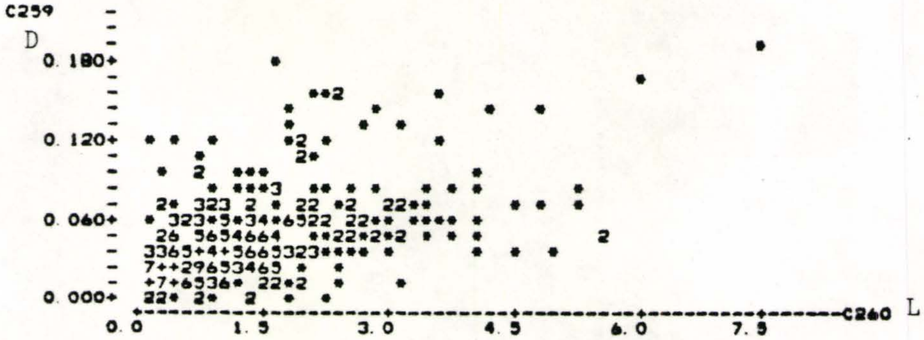

MTB > REGR C259 1 C260

The regression equation is
C259 = 0.0252 + 0.0145 C260

Predictor	Coef	Stdev	t-ratio
Constant	0.025188	0.002171	11.60
C260	0.014543	0.001224	11.88

s = 0.02789 R-sq = 25.1% R-sq(adj) = 24.9%

Analysis of Variance

SOURCE	DF	SS	MS
Regression	1	0.10981	0.10981
Error	421	0.32738	0.00078
Total	422	0.43720	

MTB > PLOT C261 C260

(d)

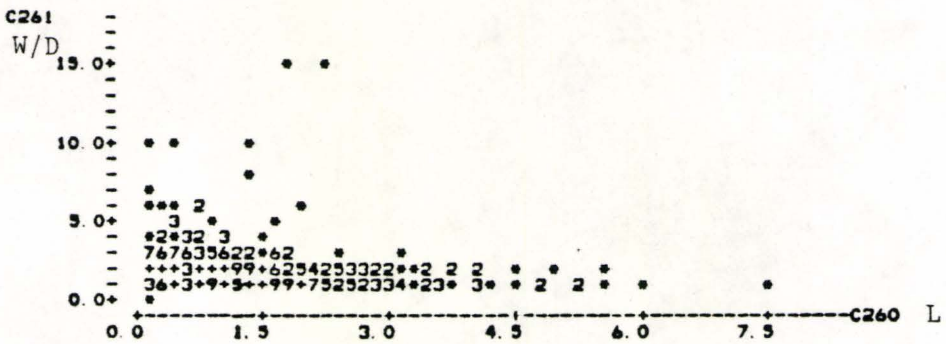

N* = 1

MTB > REGR C261 1 C260

The regression equation is
C261 = 2.37 - 0.289 C260

422 cases used 1 cases contain missing values

Predictor	Coef	Stdev	t-ratio
Constant	2.3694	0.1184	20.01
C260	-0.28863	0.06665	-4.33

s = 1.517 R-sq = 4.3% R-sq(adj) = 4.0%

Analysis of Variance

SOURCE	DF	SS	MS
Regression	1	43.157	43.157
Error	420	966.685	2.302
Total	421	1009.842	

MTB > corr c254-c257

(a)	W C254	D C255	L C256
C255	0.[illegible]44		
C256	0.8[illegible]0	[illegible]	
C257	-0.44[illegible]	-0.[illegible]	-0.441

(b)

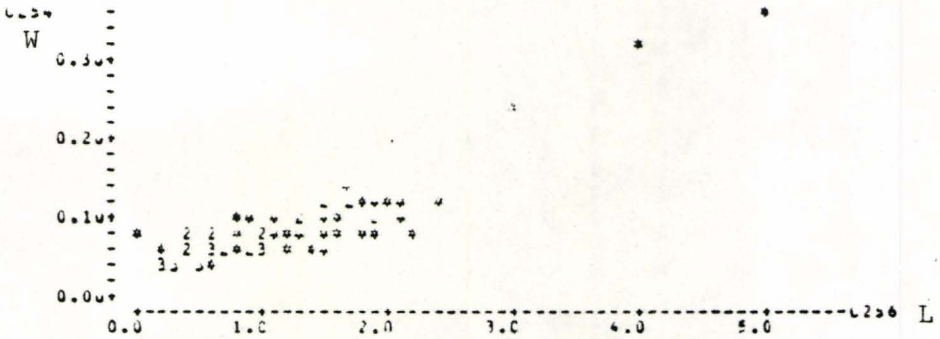

MTB > regr c254 1 c256

The regression equation is
C254 = 0.015[illegible] + 0.035[illegible] C256

Predictor	Coef	Stdev	t-ratio
Constant	0.015[illegible]	0.00[illegible]	3.5[illegible]
C256	0.035[illegible]	0.00[illegible]	15.60

s = 0.02[illegible] R-sq = 79.[illegible] R-sq(adj) = 78.[illegible]

Analysis of Variance

SOURCE	DF	SS	MS
Regression	1	0.15[illegible]	0.15[illegible]
Error	64	0.04[illegible]	0.00064
Total	65	0.19[illegible]	

Figure 3.21: Correlation (a) and regression analyses of (b) width, (c) depth and (d) w/d ratios versus length for Hortonian runnels

```
MTB > plot c255 c256
```

(c)

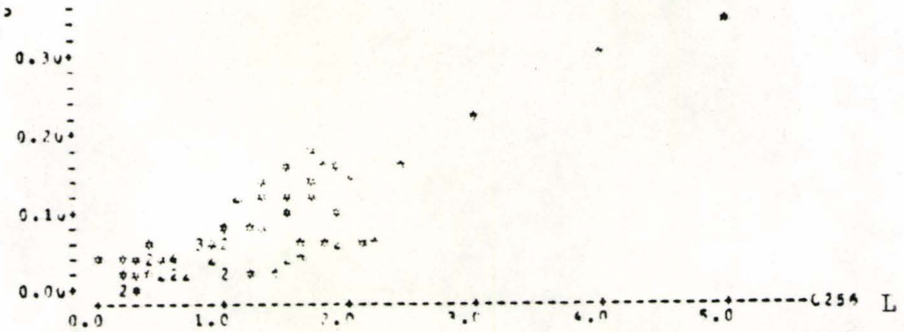


```
MTB > regr c255 1 c256

The regression equation is
C255 = - 0.0[illegible] + 0.0[illegible] C256

Predictor      Coef          Stdev       t-ratio
Constant    -0.0[illegible]    0.0[illegible]     -[illegible]
C256         0.0[illegible]     0.00[illegible]      12.57

s = 0.05[illegible]     R-sq = 71.2%     R-sq(adj) = 70.7%

Analysis of Variance

SOURCE        DF        SS          MS
Regression     1     0.[illegible]     0.2[illegible]
Error         64     0.[illegible]     0.00[illegible]
Total         65     0.[illegible]

Unusual Observations
Obs.   C256    C255      Fit   Stdev.Fit  Residual   St.Resid
  7    1.70  0.[illegible]  0.[illegible]  0.00[illegible]  0.0[illegible]   2.05R
 20    2.20  0.0[illegible]  0.1[illegible]  0.00[illegible]  -0.0[illegible]  -2.03R
 49    2.10  0.0[illegible]  0.1[illegible]  0.00[illegible]  -0.0[illegible]  -2.1[illegible]R
 62    4.00  0.[illegible]  0.[illegible]  0.014[illegible]  0.04[illegible]   1.[illegible] X
 63    5.00  0.3[illegible]  0.31[illegible]  0.01[illegible]  0.01647   0.55 X
```

```
MTB > plot c257 c256
```

(d)

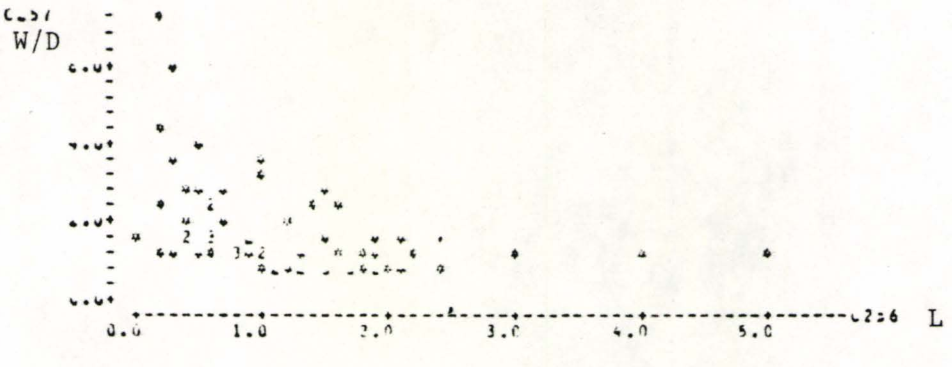


```
MTB > regr c257 1 c256

The regression equation is
C257 = 2.[illegible] - 0.5[illegible] C256

Predictor      Coef        Stdev      t-ratio
Constant     2.46[illegible]    0.2[illegible]     11.01
C256        -0.5[illegible]    0.1[illegible]     -[illegible]

s = 1.075     R-sq = 15.4%     R-sq(adj) = 14.2%

Analysis of Variance

SOURCE        DF        SS         MS
Regression     1     17.[illegible]     17.[illegible]
Error         64     73.[illegible]      1.15[illegible]
Total         65     91.73[illegible]
```

```
MTB > corr c248-c251
                 W            D            L
               C248         C249         C250
(a) C249       0.614
    C250      -0.131       -0.574
    C251      -0.014       -0.655        0.531
```

(b)

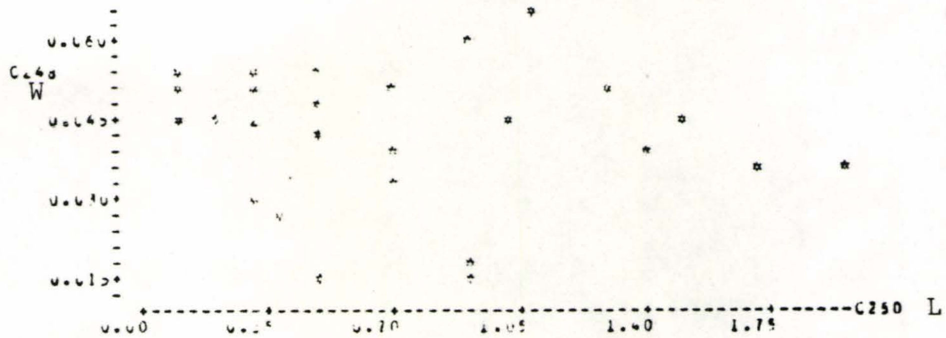


```
MTB > regr c248 1 c250

The regression equation is
C248 = 0.0445 - 0.00330 C250

Predictor        Coef          Stdev        t-ratio
Constant     0.044454       0.004310        10.27
C250        -0.003297       0.004985        -0.66

s = 0.01301      R-sq = 1.7%        R-sq(adj) = 0.0%

Analysis of Variance

SOURCE         DF          SS            MS
Regression      1      0.0000741     0.0000741
Error          25      0.0042333     0.0001693
Total          26      0.0043074
```

Figure 3.22: Correlation (a) and regression analyses of (b) width, (c) depth and (d) w/d ratios versus length for decantation runnels

(c)

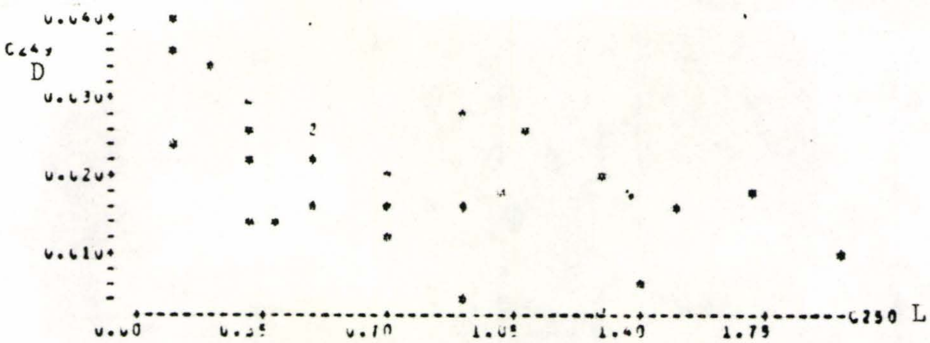


```
MTB > regr c249 1 c250

The regression equation is
C249 = 0.0276 - 0.00973 C250

Predictor       Coef         Stdev      t-ratio
Constant     0.027645     0.002429       11.38
C250        -0.009733     0.002757       -3.50

s = 0.007300     R-sq = 32.7%     R-sq(adj) = 30.2%

Analysis of Variance

SOURCE        DF         SS           MS
Regression     1   0.0006534    0.0006534
Error         25   0.0013320    0.0000533
Total         26   0.0019853
```

(d)

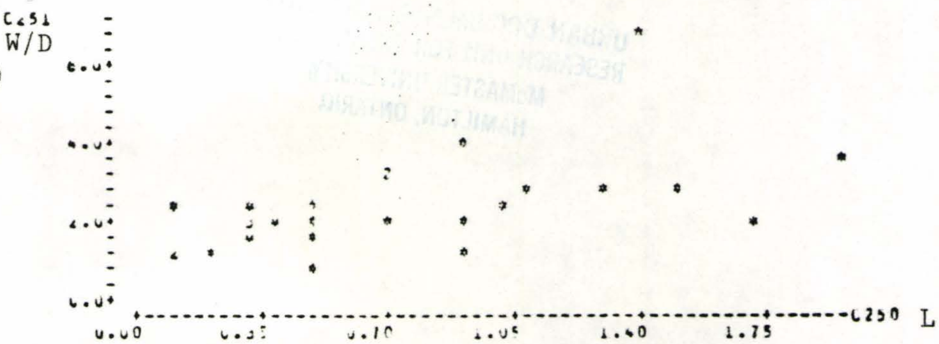


```
MTB > regr c251 1 c250

The regression equation is
C251 = 1.50 + 1.17 C250

Predictor       Coef        Stdev      t-ratio
Constant      1.5043       0.3253        4.62
C250          1.1733       0.3746        3.13

s = 0.9777       R-sq = 28.2%     R-sq(adj) = 25.3%

Analysis of Variance

SOURCE        DF          SS          MS
Regression     1      9.3782      9.3782
Error         25     23.8951      0.9558
Total         26     33.2733
```